NAVAL POSTGRADUATE SCHOOL

MONTEREY, CALIFORNIA

THESIS

DESIGN AND DEVELOPMENT OF WIRELESS POWER TRANSMISSION FOR UNMANNED AIR VEHICLES

by

Chung-Huan Huang

September 2012

Thesis Advisor:	David C. Jenn
Second Reader:	Ric Romero

Approved for public release; distribution is unlimited

THIS PAGE INTENTIONALLY LEFT BLANK

REPORT DOCUMENTATION PAGE			Form Approved OMB No. 0704–0188
Public reporting burden for this collection of information is estimated to average 1 hour per response, including the time for reviewing instruction, searching existing data sources, gathering and maintaining the data needed, and completing and reviewing the collection of information. Send comments regarding this burden estimate or any other aspect of this collection of information, including suggestions for reducing this burden, to Washington headquarters Services, Directorate for Information Operations and Reports, 1215 Jefferson Davis Highway, Suite 1204, Arlington, VA 22202–4302, and to the Office of Management and Budget, Paperwork Reduction Project (0704–0188) Washington DC 20503.			
1. AGENCY USE ONLY ***(Leave blank)***	**2. REPORT DATE** September 2012	**3. REPORT TYPE AND DATES COVERED** Master's Thesis	
4. TITLE AND SUBTITLE Design and Development of Wireless Power Transmission for Unmanned Air Vehicles		**5. FUNDING NUMBERS**	
6. AUTHOR(S) Chung-Huan Huang			
7. PERFORMING ORGANIZATION NAME(S) AND ADDRESS(ES) Naval Postgraduate School Monterey, CA 93943–5000		**8. PERFORMING ORGANIZATION REPORT NUMBER**	
9. SPONSORING /MONITORING AGENCY NAME(S) AND ADDRESS(ES) N/A		**10. SPONSORING/MONITORING AGENCY REPORT NUMBER**	
11. SUPPLEMENTARY NOTES The views expressed in this thesis are those of the author and do not reflect the official policy or position of the Department of Defense or the U.S. Government. IRB Protocol number _____N/A_____.			
12a. DISTRIBUTION / AVAILABILITY STATEMENT Approved for public release; distribution is unlimited		**12b. DISTRIBUTION CODE**	

13. ABSTRACT (maximum 200 words)

This thesis is an exploration of microwave wireless power transmission (WPT) for micro-air vehicles (MAVs). WPT, converting radio frequency (rf) power into usable direct current (dc) power, can be implemented with a rectifying antenna, or rectenna. The emphasis of this thesis is on the simulation of rectenna efficiency and measurement of experimental hardware.

In this thesis, power reflection in the rectifier matching circuit was investigated by a series of simulations using Agilent Advanced Design System (ADS). Tuning elements were added and adjusted in order to optimize the efficiency. A maximum efficiency of 57% was obtained at 10 gigahertz (GHz) with 200 mW input to the rectenna. A full-wave rectenna was built and hardware experiments were conducted to measure the efficiency of the WPT and characterize the behavior of the circuit. The design is optimized for an input power of 200 mW but, because of hardware limitations, only low-input power levels (about 1 mW) could be tested. A comparison of measurement and simulation results is given, and possible reasons for the differences are discussed.

14. SUBJECT TERMS Wireless Power Transmission, Full-wave rectenna, Schottky Diode			**15. NUMBER OF PAGES** 85
			16. PRICE CODE
17. SECURITY CLASSIFICATION OF REPORT Unclassified	**18. SECURITY CLASSIFICATION OF THIS PAGE** Unclassified	**19. SECURITY CLASSIFICATION OF ABSTRACT** Unclassified	**20. LIMITATION OF ABSTRACT** UU

NSN 7540–01–280–5500 Standard Form 298 (Rev. 2–89)
Prescribed by ANSI Std. 239–18

THIS PAGE INTENTIONALLY LEFT BLANK

Approved for public release; distribution is unlimited

DESIGN AND DEVELOPMENT OF WIRELESS POWER TRANSMISSION FOR UNMANNED AIR VEHICLES

Chung-Huan Huang
Captain, Taiwan (Republic of China) Army
B.S., Chung Cheng Institute of Technology, National Defense University in Taiwan, 2007

Submitted in partial fulfillment of the
requirements for the degree of

MASTER OF SCIENCE IN ELECTRONIC WARFARE SYSTEMS ENGINEERING

and

MASTER OF SCIENCE IN ELECTRICAL ENGINEERING

from the

NAVAL POSTGRADUATE SCHOOL
September 2012

Author: Chung-Huan Huang

Approved by: David C. Jenn
Thesis Advisor

Ric Romero
Second Reader

R. Clark Robertson
Chair, Department of Electrical and Computer Engineering

Dan C. Boger
Chair, Department of Information Science

THIS PAGE INTENTIONALLY LEFT BLANK

ABSTRACT

This thesis is an exploration of microwave wireless power transmission (WPT) for micro-air vehicles (MAVs). WPT, converting radio frequency (rf) power into usable direct current (dc) power, can be implemented with a rectifying antenna, or rectenna. The emphasis of this thesis is on the simulation of rectenna efficiency and measurement of experimental hardware.

In this thesis, power reflection in the rectifier matching circuit was investigated by a series of simulations using Agilent Advanced Design System (ADS). Tuning elements were added and adjusted in order to optimize the efficiency. A maximum efficiency of 57% was obtained at 10 gigahertz (GHz) with 200 milliwatt (mW) input to the rectenna. A full-wave rectenna was built and hardware experiments were conducted to measure the efficiency of the WPT and characterize the behavior of the circuit. The design is optimized for an input power of 200 mW but, because of hardware limitations, only low-input power levels (about 1 mW) could be tested. A comparison of measurement and simulation results is given, and possible reasons for the differences are discussed.

THIS PAGE INTENTIONALLY LEFT BLANK

TABLE OF CONTENTS

LIST OF FIGURES

LIST OF TABLES

THIS PAGE INTENTIONALLY LEFT BLANK

LIST OF ACRONYMS AND ABBREVIATIONS

ac	alternating current
ADS	Advanced Design System
BEV	battery electric vehicle
cm	centimeter
COTS	commercial off-the-shelf
CST	Computer Simulation Technology
CW	continuous wave
DARPA	Defense Advanced Research Project Agency
dB	decibel
dBm	decibels relative to a milliwatt
dc	direct current
EM	electromagnetic
ft	foot
GaAs	gallium arsenide
GHz	gigahertz
HB	harmonic balance
JAXA	Japan Aerospace Exploration Agency
kHz	kilohertz
km	kilometer
kW	kilowatt
LPF	low-pass filter
m	meter
mA	milliamp
MAV	micro aerial vehicle
METI	Ministry of Economy Trade and Industry
MHz	megahertz
mm	millimeter
mW	milliwatt
MWS	Microwave Studio
mV	millivolt

NASA	National Aeronautics and Space Administration
NPS	Naval Postgraduate School
ns	nanosecond
PCB	printed circuit board
PG&E	Pacific Gas & Electric
PtGaAs	platinum gallium arsenide
RAMP	Raytheon Airborne Microwave Platform
rectenna	rectifier antenna
rf	radio frequency
SPS	Solar Power Satellite
SSPS	Space Solar Power System
S-Parameters	scattering parameters
UAV	unmanned aerial vehicle
USEF	Institute for Unmanned Space Experiment Free Flyer
V	volt
W	watt
WPT	wireless power transmission

EXECUTIVE SUMMARY

Wireless power transmission (WPT) refers to energy transmission from one point to another without interconnecting wires. WPT can be used in a wide range of applications. One of these applications is propulsion for a micro-air vehicle (MAV), which, according to the Defense Advanced Research Project Agency (DARPA), is a fully functional unmanned aerial vehicle (UAV) no larger than 15 centimeters (cm) in length, width and height. The sustenance of flight mainly depends on the fuel capacity that an aircraft or air vehicle can carry. To conduct short range, long duration missions more efficiently, WPT applications were investigated several years ago. The concepts and technological history of WPT are presented in this thesis. The basic idea is to transfer radio frequency (rf) energy into direct current (dc) power. A rectifier plus antenna, known as a rectenna, is the device used for this function. Several rectenna studies were conducted in the past few years at the Naval Postgraduate School (NPS). The most recent studies have concentrated on a full-wave rectifier design, and a full-wave rectenna model was chosen because of its better output energy response than a half-wave rectifier design.

In this thesis, the proposed rectenna designed by a previous NPS student was re-examined. This model is designed for a fundamental frequency of 10 gigahertz (GHz) and incorporates a full-wave rectifier using HSMS 8101 Schottky diodes. In simulations, it can achieve an efficiency of 66%. The original simulation is based on ideal transmission lines without any loss. Some of these imperfections need to be addressed, such as power reflection and mismatch within the rectenna circuit.

Several Agilent Advanced Design System (ADS) simulations were conducted to examine the behavior of power reflection and to optimize the existing circuit. In order to analyze power reflection, a three-port circulator, which allows a signal to only be transmitted in one direction, was added in the simulation circuit as a diagnostic tool. An equivalent full-wave rectenna circuit with an unbalanced single-port model was developed to connect with the circulator for exploring power reflection within the circuit.

Using diode data available from the manufacturer, we optimized a full-wave rectenna for input power around 200 mW at 10 GHz with a 50 ohm load. In order to optimize the circuit, transmission line parameters were swept to find the maximum output power. In addition, all ideal transmission lines were converted to microstrip transmission lines using the LineCalc Tool for constructing the rectenna hardware. ADS simulations were conducted in both time and frequency domains. Both simulations indicate that about 20% of the incident power is reflected, which gives a return loss of 7 decibels (dB). The maximum efficiency was 54% when the input power was 0.2 W, and the estimated return loss was about 7 dB. To verify that the maximum output power occurred at 10 GHz, an efficiency response was conducted at different frequencies. At 10 GHz, the maximum output power of 0.103 W is obtained when the input power is 0.18 W, resulting in an efficiency of 57%. Further investigation demonstrated that, as the input power falls below 200 mW, the peak of the efficiency curve shifts lower in frequency.

To validate the simulation results, hardware was built based on Computer Simulation Technology (CST) Microswave Studio software. The final dipole antenna length was selected as 25 millimeters (mm) in order to obtain a good impedance match. A free space measurement was performed in the Microwave laboratory. Due to hardware limitations, the rectenna could only be tested with 1 W input to the transmit horn antenna. Consequently, the low input power to the rectenna did not allow measurement at the peak of the efficiency curve. An efficiency plot versus frequency was given for comparison with the simulated plot. The curves have similar shape, however, the maximum efficiency has shifted. For low power, both the measurement and simulations based on the measurement set up achieve their highest efficiency at a frequency lower than 10 GHz.

Efficiencies of 55 to 66 percent were predicted for various circuit designs. However, with microstrip lines, the maximum output power can be achieved when the frequency is 10 GHz with input power of 0.18 W and a conversion efficiency of 57%. The measured efficiency curve, while similar in shape, shifted lower in frequency because of the low input power. There are several possible reasons for the frequency shift. First, the ADS simulation assumes a constant source impedance. Actually, the antenna impedance changes with frequency. Any mismatch between the frequency bands of the

dipole and rectifier would not show up in the current simulation model. Secondly, the diode impedance is also assumed to the constant but is a function of frequency and input power level. Finally, an ideal free space link was assumed in calculating the received power for the measurement.

In order to get an accurate measurement of efficiency, higher input power is needed, but this cannot be obtained using a free space link with the existing amplifier. Among the recommendations is that a full-wave rectenna array and a high directivity transmit antenna be used to increase the received power. Also, a test fixture with direct power input to the rectifier circuit, that bypasses the dipole and avoids free space loss, could be used.

THIS PAGE INTENTIONALLY LEFT BLANK

ACKNOWLEDGMENTS

I would like to express my best gratitude to my country, Taiwan, and to the Chung Shan Institute of Science and Technology, Armaments Bureau, Ministry of National Defense, R.O.C., who offered me the opportunity to study at the Naval Postgraduate School.

I would like to express my sincere thanks to my advisor, Professor David C. Jenn, for his guidance on my thesis topic through these nine months. During our discussions in these days, he always provided me with different perspectives, giving me strength and encouragement to continue my studies. Without the assistance of Professor Jenn, I could not complete this research.

I would also like to thank my second reader, Assistant Professor Ric Romero, for supporting me and making correction to my thesis.

Many thanks also go to Microwave Laboratory Director, Mr. Robert Broadston. He always assisted me while I experienced technical problems during the experiments.

Finally, I want to thank my wife, Chien-Wei Chu, for her lovely support, patience and encouragement through my studies for my master's degree at the Naval Postgraduate School.

THIS PAGE INTENTIONALLY LEFT BLANK

I. INTRODUCTION

A. WIRELESS POWER TRANSMISSION

Wireless power transmission (WPT) refers to energy transmission from one point to another without interconnecting wires. There are many applications for WPT, such as wireless power charging for mobile phones, wireless power distribution systems in buildings [1] and wireless charging for battery electric vehicles (BEVs) [2]. The range for these applications varies widely [3] but can be divided into three main regions: short distance, intermediate distance and long distance.

The principle of WPT is to convert prime direct current (dc) power to radio frequency (rf) and then transmit the power by electromagnetic (EM) wave propagation. A block diagram of energy transfer is shown in Figure 1. At the receiver, there is a rectifying antenna, known as rectenna, which has the ability to convert EM waves back to direct current [4].

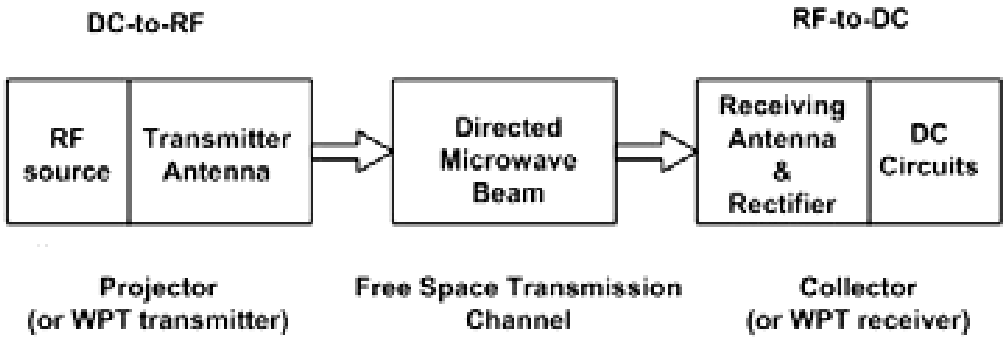

Figure 1. Wireless power transmission diagram (After [5]).

Propulsion of a micro aerial vehicle (MAV) which, according to the Defense Advanced Research Project Agency (DARPA), is a fully functional unmanned aerial vehicle (UAV) no larger than 15 centimeters (cm) in length, width and height [6], is also an important concept within the military. With microwave power, a MAV would be an

ideal way to solve the problems related to limited fuel capacity. This use of WPT provides the potential capability of a high payload fraction and allows MAVs to achieve their functions, such as communications and surveillance, for a long period of time without interruption [7]. A MAV powered by a ship's radar is illustrated in Figure 2.

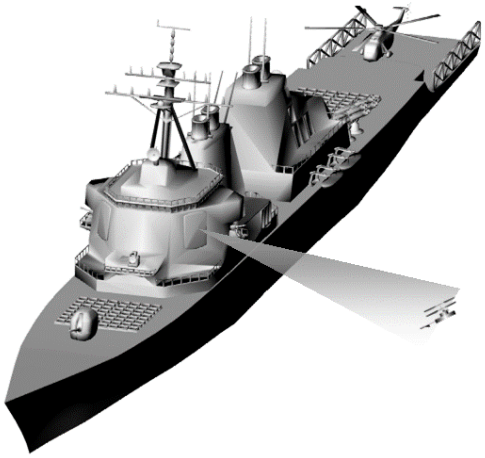

Figure 2. MAV powered by a ship's radar.

For the MAV application, it is desirable to allocate most of the system functions to the transmit side and make the receive side as simple and lightweight as possible. MAV applications can fall into either the near-field or far-field regions depending on the frequency, antenna size, and MAV operating range. The transmit side (base station) must efficiently radiate high power in the direction of the MAV. An electrically large antenna has the advantages of a narrow beam that can be pointed at the MAV. The antenna gain increases with its electrical size $D/$, where D is the aperture diameter and is the wavelength.

The full gain is realized in the far-field of the antenna. The conditions defining the far-field are illustrated in Figure 3 and given by:

$$R \gg \lambda, \tag{1.a}$$

$$R \gg D, \tag{1.b}$$

$$R > \frac{2D^2}{\lambda}. \tag{1.c}$$

If R does not satisfy these conditions, then the gain is less than the maximum.

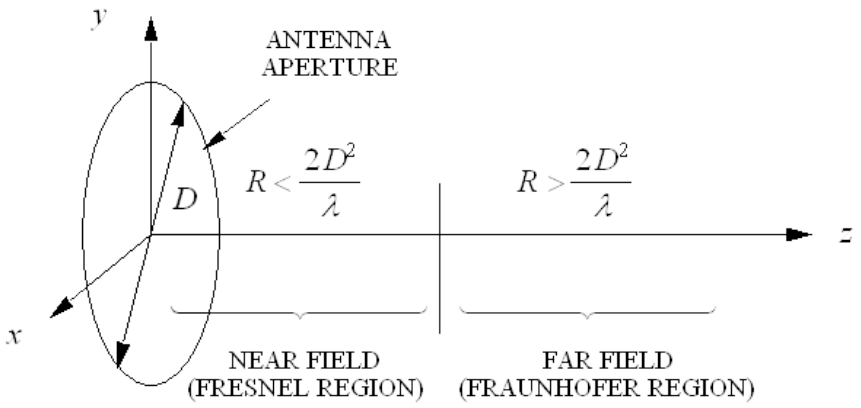

Figure 3. Illustration of the near-field and far-field regions.

Far-field power transmission generally operates in the long distance mode and can reach distances up to several decades of kilometers. The Friis equation is used in the far-field and shows that the energy transference is proportional to the inverse square of the distance. Hence, more power is required to transmit a long distance as compared to a short distance. Therefore, it is important to maximize the efficiency of the rectenna when transmitting over long distances.

In this thesis, a full-wave rectenna model based on the research and design by Liu [8] was built and tested. Various experiments and simulations were conducted to investigate the performance of the rectenna. Further improvements in the rectenna design are proposed.

B. OBJECTIVE

A full-wave rectifier circuit designed by Liu [8] claimed an output efficiency of approximately 65%, which can produce sufficient power so that a prototype MAV designed by Tsolis [6] can hover in the air. The purpose of this thesis is to test the rectenna hardware based on Liu's design, evaluate the performance of the rectenna circuit, and make changes for optimization of the rectenna system. A simulation of the complete system, including the antennas and propagation channel, is desired so that all loss sources are considered in the efficiency.

C. SCOPE AND ORGANIZATION

This thesis is divided into six chapters as follows:

The introduction and definition of WPT and MAVs are given in Chapter I, and the objective, scope and organization of the thesis are also presented.

The early history and recent developments on WPT up to the present time are given in Chapter II. References related to applications and the progress of WPT, including thesis projects conducted at Naval Postgraduate School (NPS), are also covered in this chapter.

The fundamental analysis of the full-wave rectenna is given in Chapter III. It simulates and examines the efficiency based on the circuit designed by Liu using Advanced Design System (ADS) 2011 software from Agilent Technology.

Circuit simulations for both impedance matched and mismatched circuits using transient and harmonic balance solvers are simulated in Chapter IV. Transmission line optimization is investigated and simulation results are compared with the theoretical results.

The experimental testing is examined in Chapter V. It focuses on the rectenna hardware testing and compares the measurement results to the simulation results in the previous chapter.

The findings of this research and experiments are summarized in Chapter VI. Conclusions and recommendations for the future work are also presented.

II. BACKGROUND

A. EARLY RESEARCH ON WPT

Power transmission by radio waves can be traced back to Heinrich Hertz [9] and Nikola Tesla [10–12]. In 1899, Tesla was the first to carry out experiments on power transmission, building a coil connected to a 200-foot (ft) mast with a 3-ft diameter copper ball at its top. Tesla fed 300 kilowatts (kW) into the coil, and the signal radiated out at a resonant frequency of 150 kilohertz (kHz). Unfortunately, there was no record showing how much energy Tesla received.

Later, another experiment was conducted by H. V. Noble in the Westinghouse Laboratory [13]. This experiment was set up with identical transmitting and receiving antennas, which were both half-wave dipoles at frequency of 100-megahertz (MHz), separated by a distance of about 25 ft. The outcome was that several hundred watts (W) of power were transferred between the two dipoles.

The Raytheon Company proposed the Raytheon Airborne Microwave Platform (RAMP) concept in 1959 [13, 14]. The goal was to show that it was feasible to fly a microwave-powered platform at 50,000 ft. The first demonstration of a microwave-powered helicopter (shown in Figure 4) was performed at the Raytheon Company. It was built under a contract with the Rome Air Development Center [7]. The experiment had two notable achievements. One was that helicopter flew up to ten hours by capturing the energy from the microwave beam and using it for propulsion. Secondly, the helicopter could automatically position itself by utilizing the microwave beam as the position reference. The rectenna used in this experiment is shown in Figure 5. It consisted of 4480 IN82G point of contact diodes and had a maximum output power of 270 W.

After demonstrating the first microwave-powered helicopter with point-contact diodes, Hewlett-Packard Associates suggested using silicon Schottky-barrier diodes (Type 2900), which have better performance than the point-contact diodes. Tests showed

that Schottky-barrier diodes are much more efficient and have the advantage of smaller size [13]. From that time on, the Schottky diode became a critical component within the rectifier circuit.

Figure 4. Experiment for microwave-powered helicopter (From [7]).

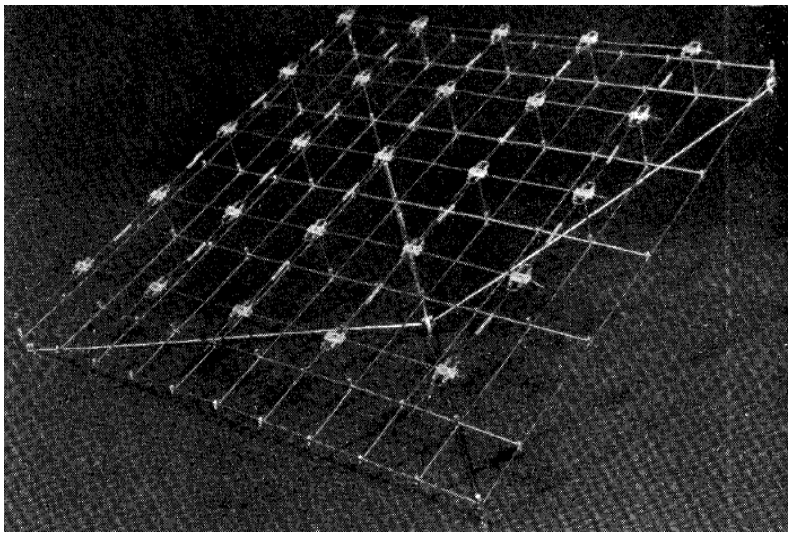

Figure 5. First rectenna made for the microwave-powered helicopter (From [13]).

B. RECENT AND EXISTING DEVELOPMENT ON WPT

As WPT technology matured in the late 20th century, a means of exploiting solar energy was proposed by Dr. Peter Glaser [15]. Base-load electrical power would be provided by using the photovoltaic cell principle and converting the sun's energy collected at a satellite into microwave power. The microwave power is then beamed to Earth, where it is converted back into ordinary electrical power [16]. The Space Solar Power System (SSPS), shown in Figure 6, consists of a Solar Power Satellite (SPS) and a ground power facility. Within the SSPS, the solar cells are used to collect the solar energy in space and must be directed toward the sun in order to get the maximum power input. With respect to the microwave power transmission process, the antenna must be directed toward the Earth, and the ground rectifying antenna would collect the microwave beam and convert it to electricity.

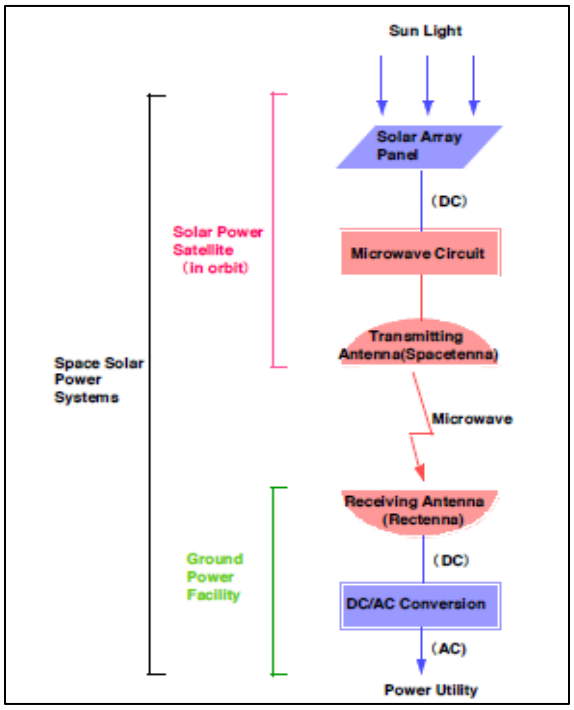

Figure 6. Configuration diagram of SSPS (From [17]).

More research was conducted by the National Aeronautics and Space Administration (NASA) by sponsoring a study of the SPS through its Lewis Research

Center in the 1970s [18]. Under this SPS study, a demonstration experiment of WPT for SPS application was conducted in 1975, using a 7.3 meter (m) high by 3.5 m wide matrix array, which was separated by a distance 1.54 kilometers (km) at an elevation angle of 7 degrees from a 26 m parabolic diameter antenna. The outcome showed that 30 kW was obtained at a receiver when transmitting 450 kW continuous wave (CW) power at 2.388 gigahertz (GHz) [19].

Although NASA had confirmed the feasibility of an SPS, it was concluded that the concept was not economical based on the technology of the time [20]. More recently, a "Fresh Look" study of the concept was performed by NASA in 1995 [21], which checked innovative concepts that differed from previously examined concepts and technologies in order to reduce the cost. Several economic analyses were conducted, based on market goals and system tradeoffs, relying on existing data. Finally, in 2009, Pacific Gas and Electric (PG&E) signed a contract to buy power from an SSPS startup company, Solaren Corp., that would begin operating in 2016 [22].

Japan has pursued further investigations on SPS and related technologies [23]. Two major SPS models are depicted in Figure 7. One of the SPS designs was produced by the Japan Aerospace Exploration Agency (JAXA), and the other is a tethered-SPS [24] designed jointly by the Japanese Ministry of Economy, Trade and Industry (METI) and the Japanese Institute for Unmanned Space Experiment Free Flyer (USEF).

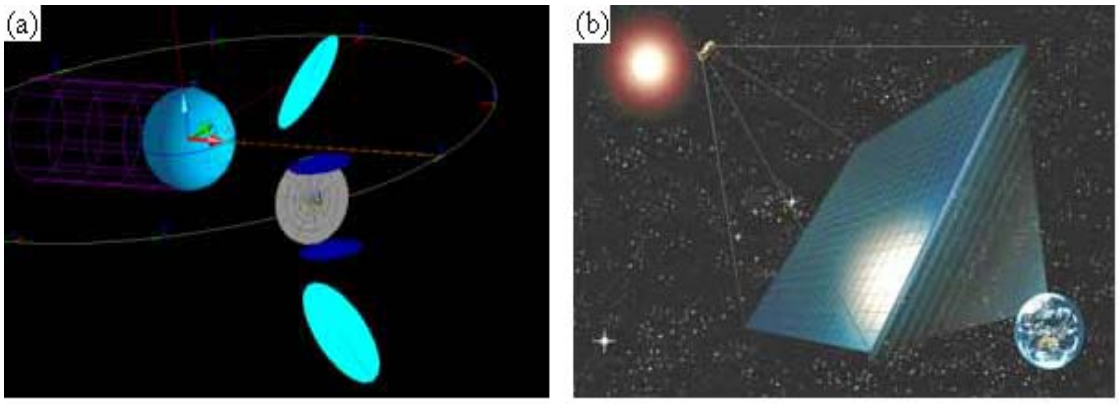

Figure 7. Recent SPS designs in Japan (a) JAXA-SPS (b) USEF-SPS (From [23]).

These aforementioned projects are just a few of the many that were conducted up to now, but most of the concepts use microwave WPT, rather than laser, due to the fact that microwaves produce a higher efficiency at both the transmitter and receiver sides and a lower atmospheric attenuation.

C. PREVIOUS WORK ON RECTENNAS

W. C. Brown [13] was the first person to introduce the term rectenna (rectifying antenna) and developed the first rectenna in 1963. It was built and tested by R. H. George at Purdue University and had an efficiency of 50% at an output power of 4 W and an efficiency of 40% at an output power of 7 W. It operated at frequency of two to three GHz. In the following years, Brown reported a 90% conversion efficiency rectenna using platinum gallium arsenide (PtGaAs) Schottky diodes with an input power of 8 W [25] and 85% conversion efficiency with thin-film rectenna arrays at 2.45 GHz [26], which was subsequently verified [27].

In order to achieve a higher output power with a rectenna array, research into connecting rectennas in series or parallel configuration was conducted in 1979 using both a closed-form analytical circuit model and computer simulation model [28]. Shinohara and Matsumoto [29] showed that the sum of the dc output power with an antenna array in parallel connection is larger than for a serial connection.

In 1992, Yoo and Chang [30] presented the efficiency of gallium arsenide (GaAs) Schottky diodes (Model DMK6606) in a closed-form equation, which was used for the high frequency rectenna analysis, neglecting the higher order harmonics. The conversion efficiency achieved was 39% and 60% at frequency 35 GHz and 10 GHz, respectively.

At 35 GHz, a high-efficiency rectenna array was designed consisting of 1000 dipole elements using a silicon Schottky diode quad bridge. The efficiency exceeded 80% at 5.87 GHz [31]. McSpadden continued the work and reported an 82% efficiency rectenna using silicon Schottky barrier mixer diodes at 5.8 GHz, at an input power of 50 milliwatts (mW) in 1998 [32].

Within the concept of a dual polarized patch rectenna introduced by McSpadden and Chang [33], Suh and Chang [34] designed a dual frequency printed dipole rectenna,

operating simultaneously at 2.45 and 5.8 GHz. For operating in dual bands, a GaAs Schottky barrier diode has been employed in order to achieve the optimum input impedance and load impedance. With such an approach, efficiencies of 84.4% and 82.7% were achieved at 2.45 and 5.8 GHz, respectively.

Since system requirements limit antenna size and weight, fractal antennas were investigated by Werner and Ganguly [35] due to their unique properties and compact size. This topic was further investigated by Mohammed [36] in 2010, using the Sierpinski carpet edge-fed microstrip-patch fractal antenna. The result was that the size of the antenna was reduced 27.68% at 2.45 GHz without affecting performance measures such as return loss and radiation pattern.

D. NPS PROJECT

Students at NPS have been studying WPT for MAV propulsion since 1999. Vitale [37] designed a rectifier system to power a remote MAV at frequencies of 1.0 GHz and 1.3 GHz using a semi-omni-directional antenna with less than 2 W of transmitted power. He demonstrated that it is possible to power a remote vehicle through WPT but achieved a conversion efficiency of only 33% by using commercial-off-the-shelf (COTS) hardware.

Tsolis [6] extended Vitale's work by using a Schottky barrier diode (HSMS 8101) due to its high switching capability. A rectenna array consisting of circular patch antennas was tested, with 8.2% conversion efficiency for total circuit. The low efficiency was due to a mismatch between the antenna frequency and filters employed in the circuit.

Tan [38] did more research on the rectenna array, proposing a round patch antenna instead of a circular patch antenna introduced by Tsolis and a sixth-order pre-rectification Butterworth filter. The final size of the rectenna designed by Tan was reduced by 15% of the previous design. Tan also re-evaluated the use of Schottky diodes and projected an efficiency of 60%.

Toh [39] built a 4 x 4 rectenna array where the efficiency of each single rectenna element varied between 26% and 37%. However, the total efficiency did not come out as expected, and the output power was insufficient for the MAV motor to hover for an input power of 23 decibels per milliwatt (dBm) transmitted by a nearby horn antenna.

Liu [8] modeled two different rectenna designs using Agilent ADS software: a half-wave rectenna and a full-wave rectenna. A full-wave rectenna without a low-pass filter was chosen because of the low weight and had a simulated conversion efficiency of 66%. He also used a dipole antenna instead of circular patch antenna because the dipole antenna is much lighter. Liu recommended that further analysis on antenna array be done and a hardware prototype built to verify the efficiency.

E. SUMMARY

In all of the NPS efforts, the efficiencies achieved were low compared to values predicted by simulation. As will be seen in later chapters, the optimum circuit design depends on the diode impedance match and motor resistance. Both of these are known only approximately, and furthermore, they are a function of power level.

In the next chapter the basic requirements of the rectenna are presented.

THIS PAGE INTENTIONALLY LEFT BLANK

III. RECTENNA SYSTEM DESIGN

A. BASIC RECTENNA STRUCTURE

The rectenna consists of several sub-systems. Typically, it can be separated into four main components: antenna, pre-rectification filter, rectifier and post-rectification filter. A block diagram of a basic configuration of rectenna diagram is shown in Figure 8. A brief description of each block follows.

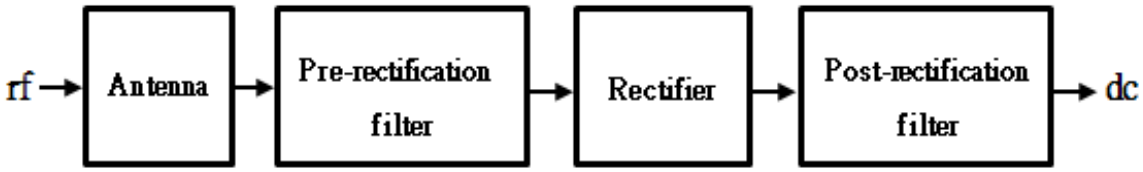

Figure 8. Generic rectenna system configuration (After [39]).

1. Antenna

The antenna is used to collect rf power and transfer the energy to the pre-rectification filter. There are several kinds of antennas that can be used, such as a dipole, dish, horn, etc. The main factors in the antenna design are its gain pattern at the operating frequency, size and weight of the antenna, and its return loss.

2. Pre-rectification Filter

The pre-rectification filter allows certain frequencies of the incoming rf signal to pass through the filter and ensure that the incoming signal is within the desired operating band. It also prevents the re-radiation of higher-order harmonics produced by the non-linear *I-V* characteristics of the diode.

3. Rectifier

The rectifier is perhaps the most important component within the rectenna, converting incoming rf power to dc. It usually consists of a diode with a high switching speed and high-power handling characteristics. Diode *I-V* characteristics, operating

frequency impedance, forward bias voltage, breakdown voltage, and saturation current also need to be taken into consideration while designing the rectifier.

4. Post-rectification Filter

The post-rectification filter performs a similar function to the pre-rectification filter, allowing the desired frequency signal to the output and preventing the unwanted frequencies (harmonics) from appearing in the output voltage.

B. PREVIOUS DESIGN AND SIMULATION

Students at NPS have simulated several types of rectennas, such as a circular patch rectenna, square patch rectenna, hybrid rectenna, half-wave rectenna and full-wave rectenna [8, 38, 39]. Generally, the operating frequency is at 10 GHz. According to the diode characteristic measurement in Table 1, the Schottky diode (HSMS8101) has a maximum output power at this frequency [39]. Based on this frequency, Liu [8] suggested using a full-wave rectenna and simulated a best conversion efficiency of 66%.

Table 1. Measured data for the HSMS8101 diode characteristic (From [39]).

Frequency	Current (mA)	DC Voltage (V)	Power (mW)
9.00	-2.36	-2.01	4.74
9.10	-2.13	-2.51	5.35
9.20	-2.78	-1.70	4.73
9.30	-3.16	-1.38	4.36
9.40	-3.38	-1.14	3.85
9.50	-4.65	-1.12	5.21
9.60	-8.72	-1.15	10.03
9.70	-13.02	-1.92	25.00
9.80	-13.85	-2.31	31.99
9.90	-11.92	-2.85	33.97
10.00	-11.40	-3.61	41.15
10.10	-9.81	-3.91	38.36
10.20	-8.31	-3.83	31.83
10.30	-7.31	-3.62	26.46
10.40	-3.81	-2.62	9.98
10.50	-2.21	-1.54	3.40
10.60	-1.51	-1.10	1.66
10.70	-0.81	-0.68	0.55
10.80	-0.61	-0.38	0.23
10.90	-0.44	-0.41	0.18
11.00	-0.36	-0.40	0.14

1. Rectifier

The characteristics of the diode, such as recovery time, forward resistance, reverse resistance and barrier capacitance, affect the efficiency of the rectenna. Due to its low capacitance, low conversion loss, and fast switching speed, Tsolis [6] decided to use Agilent HSMS 8101 Sckottky Barrider diode as the main component for rectification.

2. Full-wave Dipole Antenna

In order to reduce the overall weight of the rectenna, a dipole was chosen over other antenna types. Liu calculated the efficiency of the full-wave, half-wave and hybrid rectennas. Results indicated that the full-wave rectenna shown in Figure 9 can achieve a better efficiency than the other two types. The full-wave rectenna consists of two diodes and, thus, can get a higher average output dc voltage than the half-wave rectenna. The full-wave rectenna has the advantage of using every half-cycle of the input voltage instead of every other half-cycle. From Figure 9, we can easily see that the full-wave rectifier has a better output energy response than the half-wave rectifier.

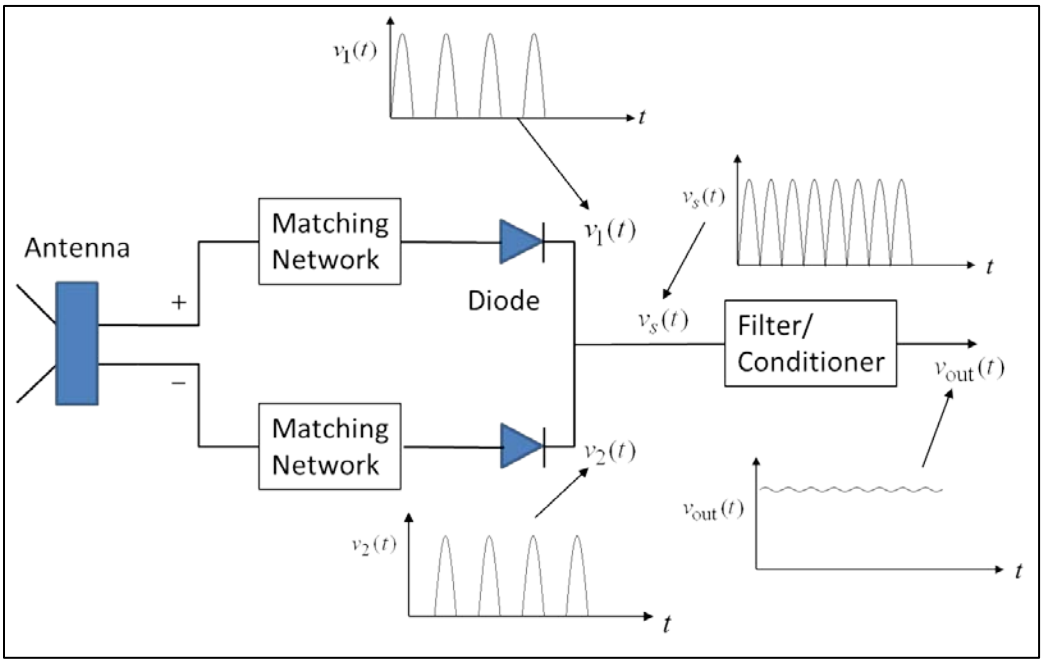

Figure 9. Full-wave rectifier output response for a sinusoidal input.

3. Rectification Filter

Liu [8] performed three different simulations: (1) a low-pass filter (LPF) before the Sckottkky diode, (2) an LPF after the diode and (3) without a filter. From Figure 10, it can be seen that both the efficiency plot of the full-wave rectenna with post-LPF and no-LPF have similar curves, which are higher than the pre-LPF design. The efficiency of the full-wave rectenna without LPF can achieve 66% at an input power of 200 mW (23 dBm).

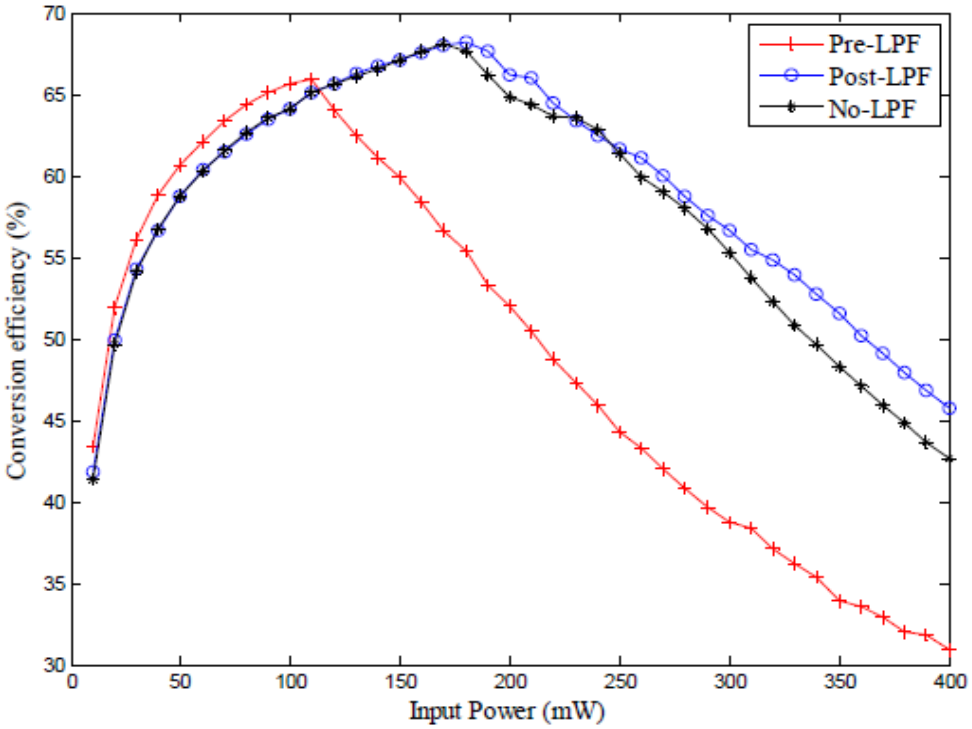

Figure 10. Full-wave rectenna efficiency plot with different LPF positions (From [8]).

Therefore, Liu concluded that full-wave rectenna with either post-LPF or no LPF can have a better performance compared to pre-LPF rectenna. In order to get the impedance match of the whole circuit and reduce the weight, Liu added microstrip lines into the full-wave rectenna circuit with no LPF. The final design is shown in Figure 11.

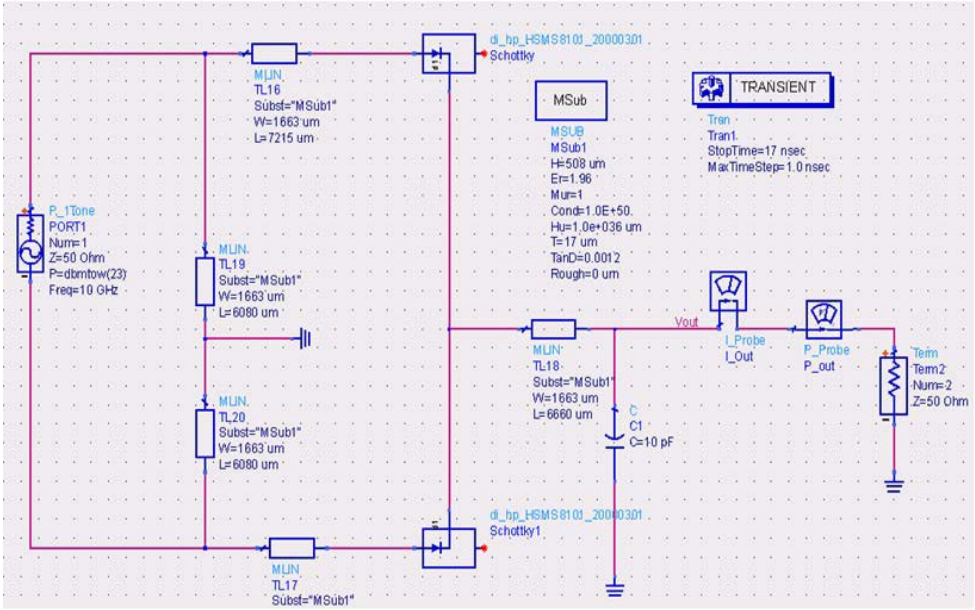

Figure 11. Full-wave rectenna circuit designed by Liu (From [8]).

To verify Liu's design, an efficiency test was simulated using ADS 2011 for both ideal transmission lines and microstrip transmission lines. The efficiency plots are shown in Figure 12 and Figure 13.

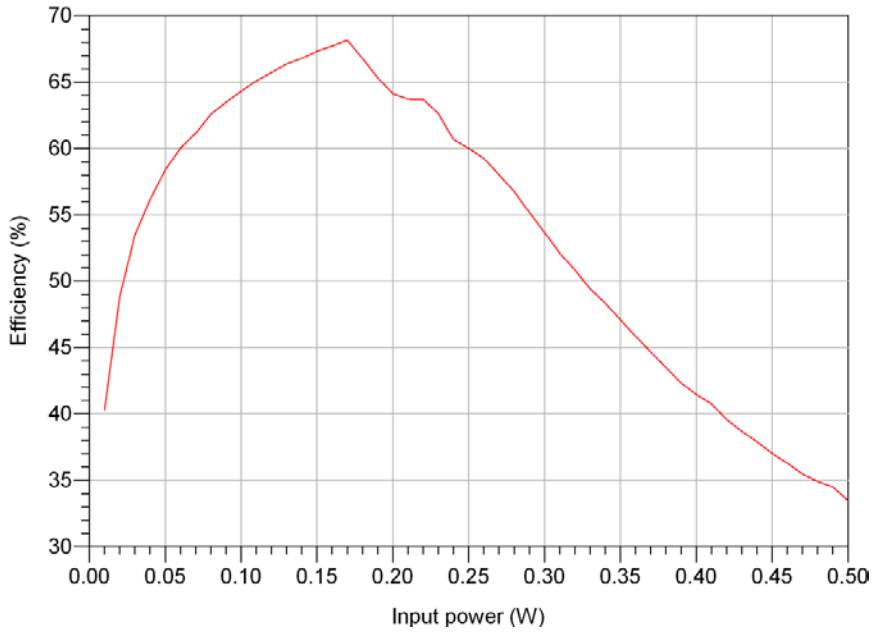

Figure 12. Full-wave rectenna efficiency using ideal transmission lines.

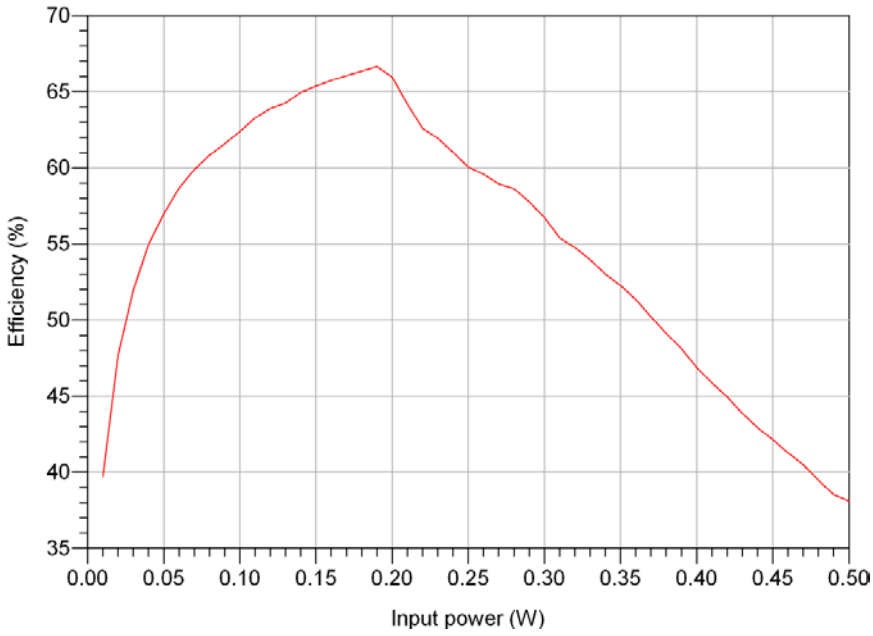

Figure 13. Full-wave rectenna efficiency using microstrip transmission lines.

The parameters used for the microstrip substrate are shown in Table 2. With the ideal transmission line circuit, we get a full-wave rectenna efficiency of 64% as indicated in Figure 12; with the microstrip transmission line circuit, we get an efficiency of 66% as in Figure 13. The two results are very similar to what Liu claimed in his thesis, which is 66%.

Table 2. Parameters using in microstrip substrate simulation.

Substrate thickness (H)	508 μm
Dielectric constant (ε_r)	1.96
Relative permeability ( )	1
Conductor conductivity	10^{50} (Siemens/m)
Cover height	10^{36} μm
Conductor thickness	17 μm
Dielectric loss tangent	0.0012

C. SUMMARY

When designing the rectenna, we need to take several factors, such as weight, power supply, impedance match, etc., into consideration. An important part of the design is the matching unit, which minimizes power reflection. In this chapter, a full-wave rectenna was analyzed, and the operation was simulated using ADS 2011. A multiparameter sweep was used to optimize the efficiency, which achieved a maximum value of 66%.

In the next chapter, power reflection and efficiency are simulated, and a rectenna simulation using ADS is presented for comparison.

THIS PAGE INTENTIONALLY LEFT BLANK

IV. SIMULATION

In this chapter, several rectenna simulations are investigated in both time and frequency domains using Agilent ADS software for electronic circuits, power and systems research. Transmission line optimization and efficiency response at different frequencies are also computed in the ADS simulations.

A. BACKGROUND

Agilent ADS is an electronic circuit simulation software application that can model circuits in both the time and frequency domains. In the time domain, both voltage and current vary with time at each point throughout the circuit. On the other hand, the frequency domain obtains voltage, currents and power as a function of frequency over a prescribed bandwidth. Users can select from a complete range of components in libraries and construct any desired circuit or system. Users can sweep parameters by simply assigning a variable to different quantities, such as input power, frequency, time and so on. These sweep plans can provide a complete picture of circuit performance in non-ideal cases because ADS includes all higher order effects such as reflections, losses, and intermodulation.

B. SIMULATION

To begin with, several simple circuits are simulated to examine the ADS outputs and compare several approaches to modeling the rectifier circuits. We compare results for the transient simulation (time domain) and the harmonic distortion analysis (frequency domain).

1. Balanced vs. Unbalanced Source

Liu's simulation [8] used a balanced source that accurately represents the dipole antenna as a voltage source. The voltage source's positive and negative terminals each drive a branch of the full-wave rectifier (Figure 11). The voltage source in Figure 14 represents an unbalanced feeding method. The positive terminal feeds a power splitter whose outputs feed a rectifier branch. This model represents the case when the antenna

output might be a coaxial cable. The efficiency shown in Figure 15 is essentially the same as that shown in Figure 13. Therefore, the two feed models give similar results, as expected. The maximum efficiency is at a slightly different input power (shifted to 0.15 W).

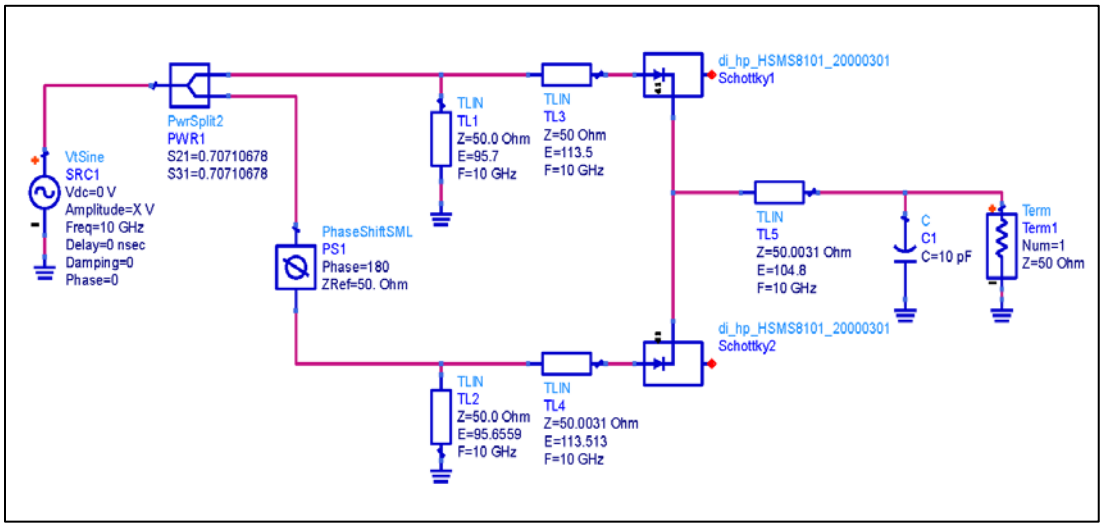

Figure 14. Unbalanced source port rectenna circuit.

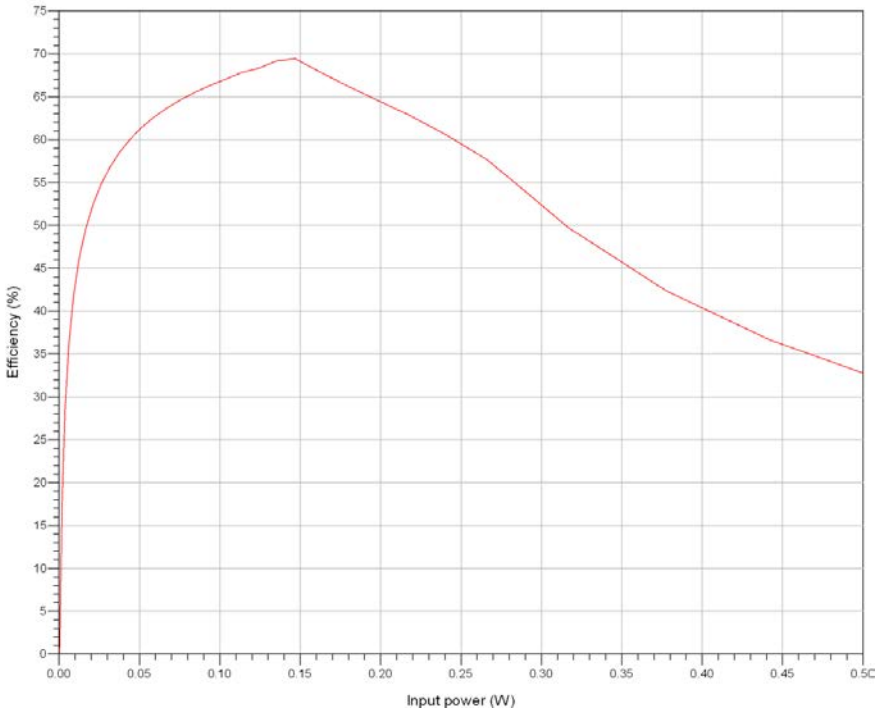

Figure 15. Efficiency plot for unbalanced source rectenna.

In the following sections, both time and frequency domains are simulated both when the impedance is matched and when it is mismatched to examine the power reflections in the circuit. Probes are placed at positions throughout the circuit to see the reflected power at various points. Circulators are inserted to isolate flow in certain directions for comparison with the probes.

2. Transient Simulations

A transient simulation is performed entirely in the time domain and is unable to explain frequency-dependent behavior. Power, voltage and current measurements are instantaneous values. All measurements can be analyzed at different times; however, peak values are chosen in order to simplify the calculation.

A voltage source defines an alternating current (ac) sinusoidal waveform generator and is chosen for the time source simulation. Voltage can be expressed as an exponentially damped sine wave as follows:

$$V(t) = V_{dc} + \text{Amplitude} \times \sin\left[2\pi \left(\text{Frequency}\left(t - \text{Delay}\right) + \frac{\text{Phase}}{360} \right) \right] \times e^{-(t-\text{Delay})\times\text{Damping}} \quad (4.1)$$

where V_{dc} is the initial voltage offset, *Amplitude* is the amplitude of the sinusoidal wave, *Frequency* is the frequency of the sinusoidal wave, *Delay* is time delay, *Damping* is the damping factor, and *Phase* is the phase value of the sine wave. To simplify the input sinusoidal signal, the initial voltage offset, time delay, damping factor and phase are all set to zero. With an amplitude of 10 V and a frequency of 10 GHz,

$$V(t) = 10\sin\left(2\pi \times 10^{10} t\right). \quad (4.2)$$

For transient simulations, an observation start time of 10 nanoseconds (ns) is selected to avoid transients. An impedance matched circuit with 50 ohm loads is shown in Figure 16. The simulation verifies that there are no reflections when the impedances are matched. By changing one of the loads to 100 ohms, power reflection can be calculated and compared to simulation results. The mismatched circuit is shown in Figure 17.

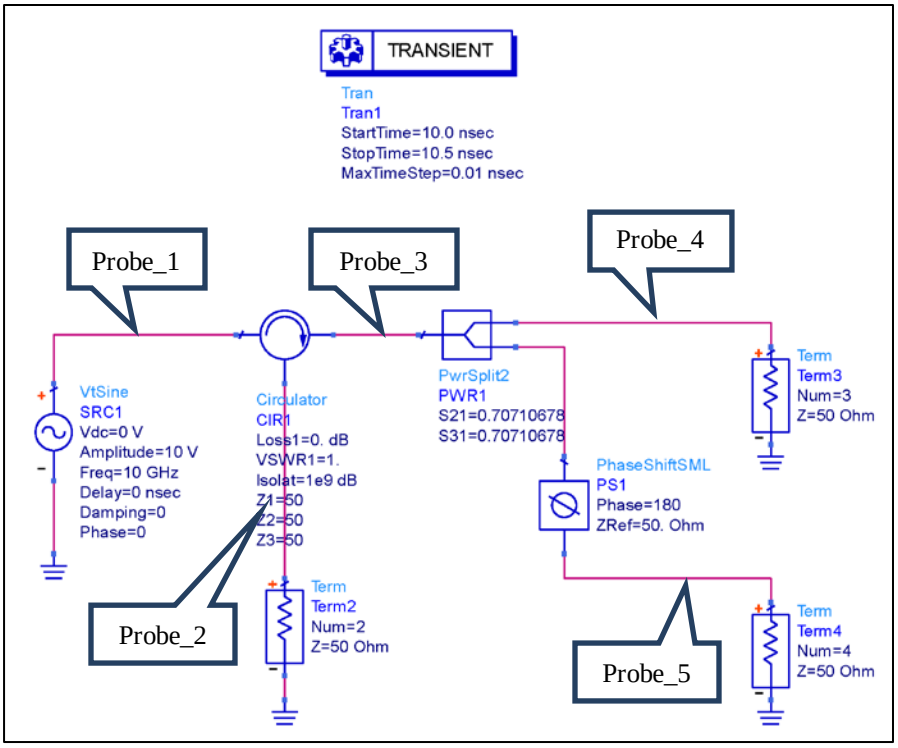

Figure 16. Transient simulation for impedance matched circuit.

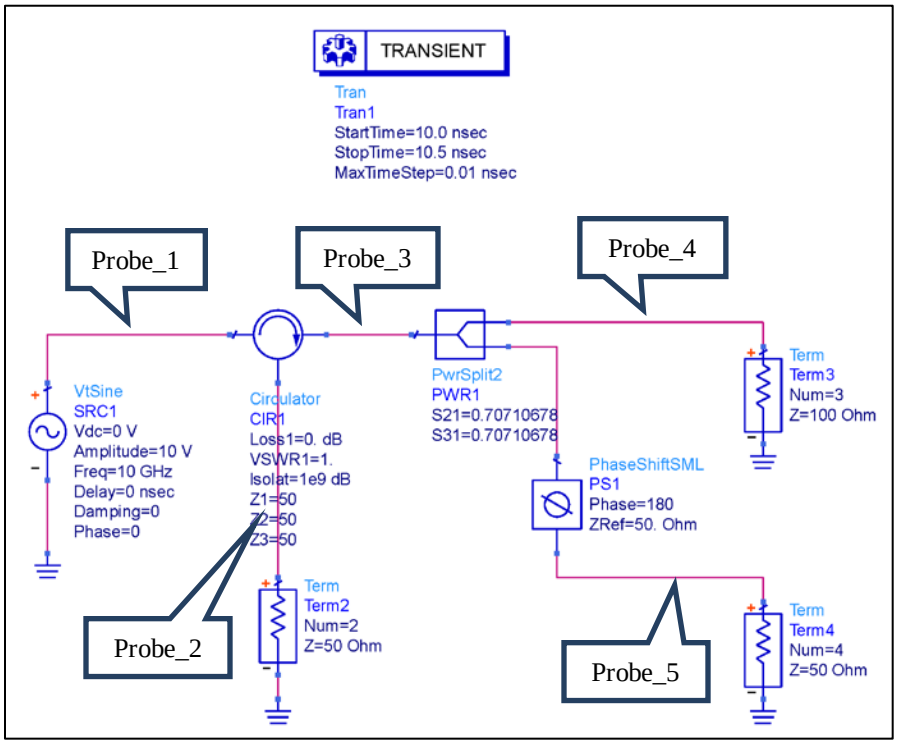

Figure 17. Transient simulation for impedance mismatched circuit.

The simulated power at different points for both impedance matched and mismatched circuits are shown in Figure 18 and Figure 19. Probe_1 is the incident input power, Probe_2 is the power reflected back to the source, Probe_3 is the power transmitted to the power splitter, and Probe_4 and Probe_5 are the powers transmitted to the two loads.

In Figure 18, the curves for Probe_4 and Probe_5, overlap, as do the curves for Probe_1 and Probe_3, and the amplitude is half of the input power. As expected, there is no power reflection with an impedance matched circuit. However, referring to Figure 19, it is evident that powers after the splitter are not equal. This is due to the fact that mismatches cause some power to be reflected back to the source.

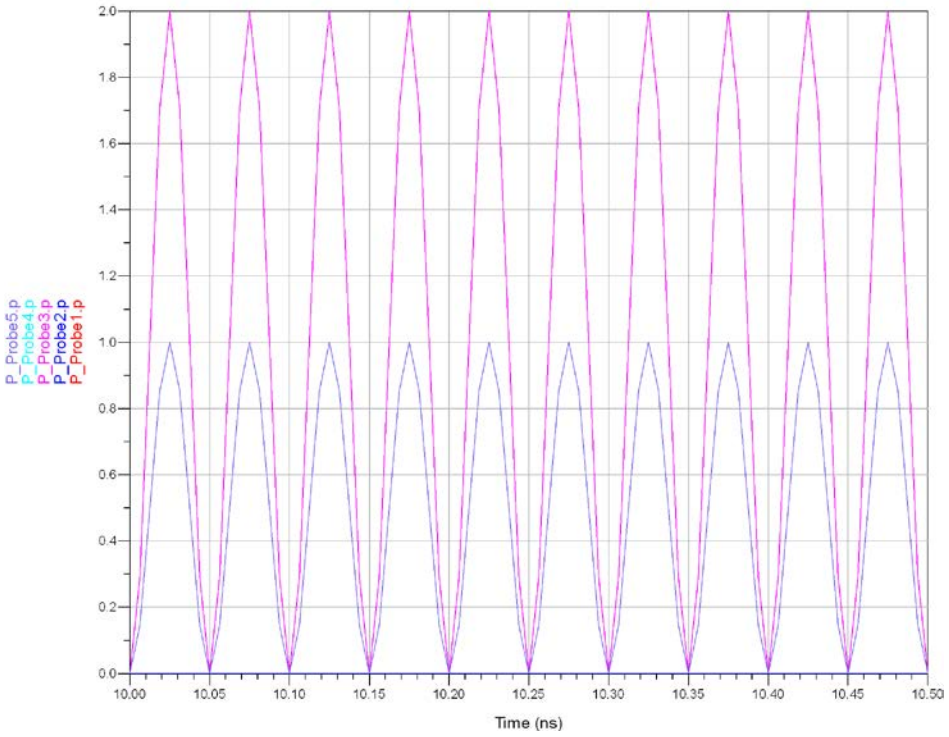

Figure 18. Simulated power for the matched circuit.

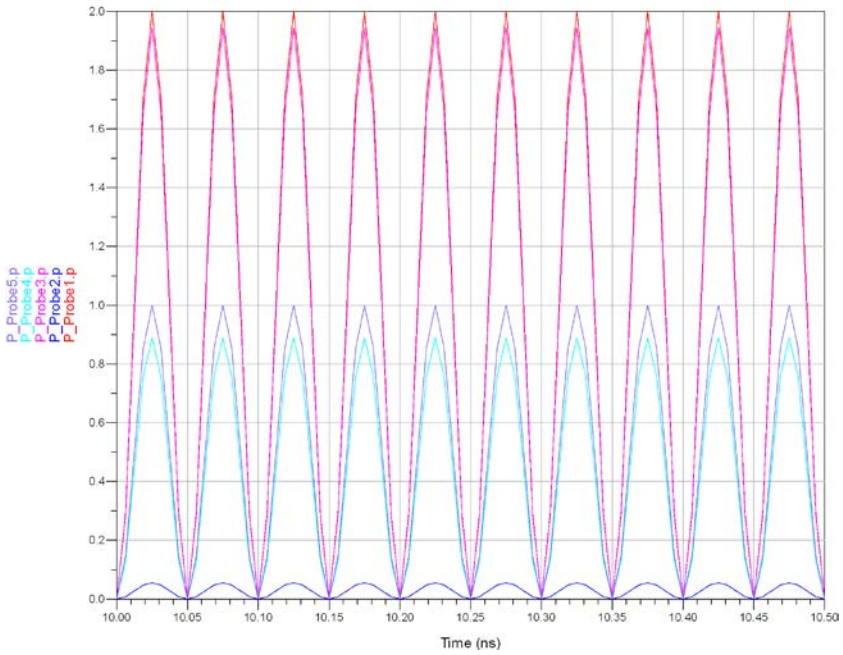

Figure 19. Simulated power for the mismatched circuit.

From Figure 18 and Figure 19, it can be seen that at time 10.025 ns, the peak values appear. The values are recorded in Table 3 for comparison with calculated results.

Table 3. Peak power results for different loads.

Probe	Power measured in matched circuit (W)	Power measured in mismatched circuit (W)
Probe_1	2	2
Probe_2	≈0	0.05556
Probe_3	2	1.94444
Probe_4	1	0.88889
Probe_5	1	1

Based on [40], the reflection coefficient at a load can be calculated as

$$\Gamma = \frac{Z_L - Z_0}{Z_L + Z_0} \tag{4.3}$$

where Z_L is load impedance, and Z_0 is line's characteristic impedance. Thus, the reflection coefficient at Terminal 3 for the mismatched circuit equals 1/3. The transmitted power can be calculated since it is equal to the average incident power, diminished by a multiplicative factor of $|\Gamma|^2$ as shown in Figure 20. Since

$$P_{av}^r = |\Gamma|^2 P_{av}^i \tag{4.4}$$

the transmited power is given by

$$P_{av}^t = P_{av}^i - P_{av}^r = P_{av}^i \left(1 - |\Gamma|^2\right). \tag{4.5}$$

Thus, the reflected power is 0.11111 W, while the incident power is 1 W. So the net power through Probe_4 is the same value as in Table 3: 0.88889 W.

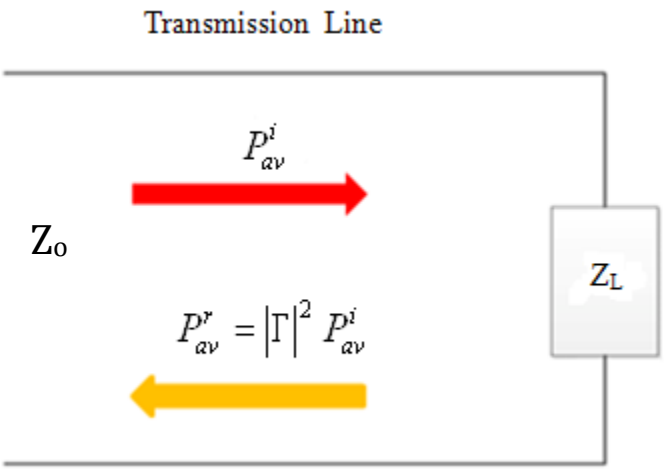

Figure 20. Power reflection at a terminated transmission line.

Since a power splitter can be regarded as a resistive power divider, its scattering matrix is [41]:

$$[S] = \frac{1}{2}\begin{bmatrix} 0 & 1 & 1 \\ 1 & 0 & 1 \\ 1 & 1 & 0 \end{bmatrix}. \tag{4.4}$$

Thus, S_{12} equals to 1/2, which shows that the reflected power going back to the input port is half of the reflected power. A reflected power flow diagram is presented in Figure 21. The power back to Probe_2 is half of the reflected power in Probe_4: 0.05556 W. Probe_3's power can be calculated by subtracting 0.05556 W from the input power. The simulated results all correspond to the theoretical values.

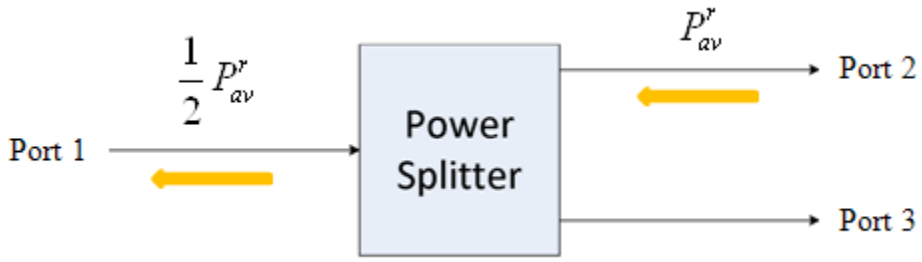

Figure 21. Power flow diagram for the power splitter.

3. Harmonic Balance Simulation

Harmonic balance (HB) is a frequency domain analysis for simulating distortion in nonlinear circuits. The simulation requires at least one fundamental frequency. In this case, 10 GHz is the fundamental frequency, with five orders (harmonics) used in the ADS simulation. The advantage of using the HB simulation over conventional transient analysis is that HB can calculate the steady-state spectral content of voltages or currents in the circuit. Furthermore, power distribution over a range of frequencies can be seen in the simulation results.

Unlike the time source, the frequency source is specified by power, frequency and impedance. Power is simply set at the fundamental frequency, and the internal impedance is set to 50 ohms in order to match the circuit. The frequency source output waveform is a cosine; thus, the initial phase is set to minus 90 degrees in order to get a same signal as the transient simulation. The simulation circuits with frequency sources for the different impedance loads are shown in Figure 22 and 23.

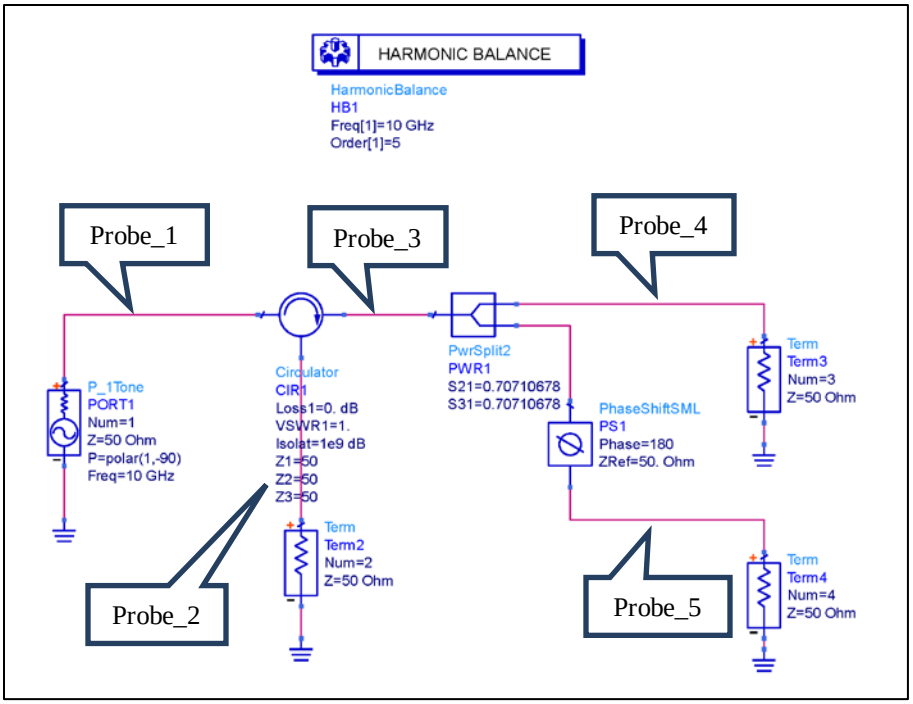

Figure 22. Harmonic balance simulation for the impedance matched circuit.

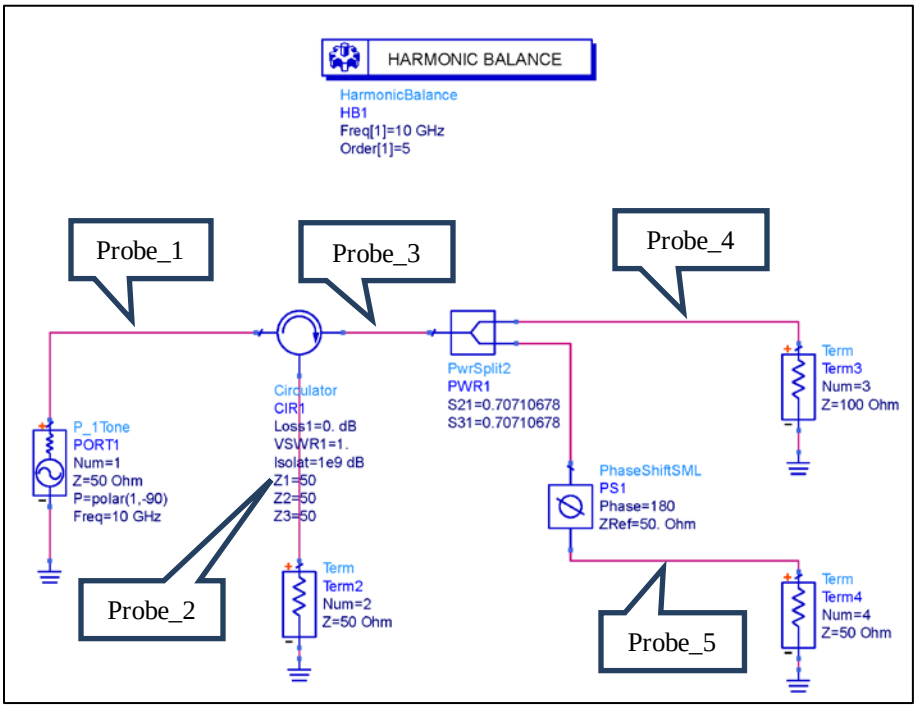

Figure 23. Harmonic balance simulation for the impedance mismatched circuit.

The simulated power spectra are presented in Figure 24 and Figure 25. Due to the large axis range in Figure 24, several of the stems are not visible, so the values are recorded in Table 4. From Table 4, it can be seen that power levels for both Probe_4 and Probe_5, and similarly for Probe_1 and Probe_3, have the same amplitude, but the levels are not the same in Figure 25. This corresponds to the transient simulation, showing that there are some power reflections in the mismatched circuit.

The difference between the time and frequency simulations is that the power we get for HB is an average value, not instantaneous. Therefore, the power results for the transient simulation are twice those for the harmonic balance simulation.

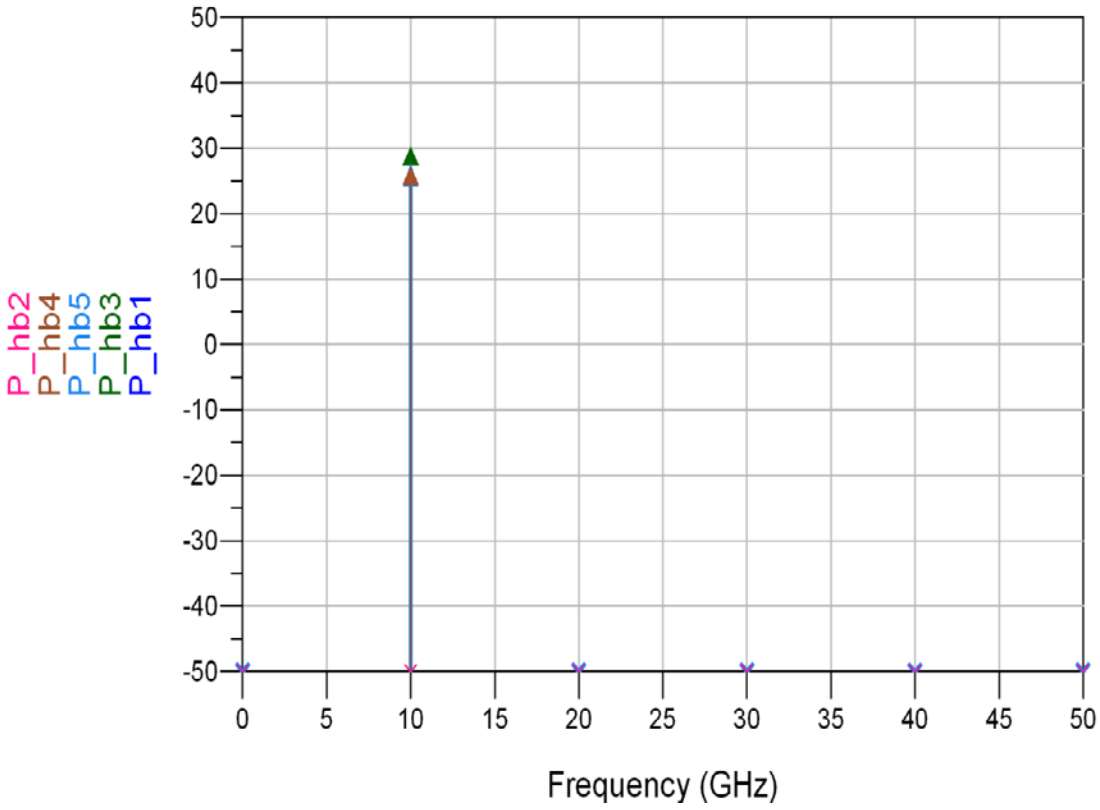

Figure 24. Simulated power spectra at five probe locations for the matched circuit.

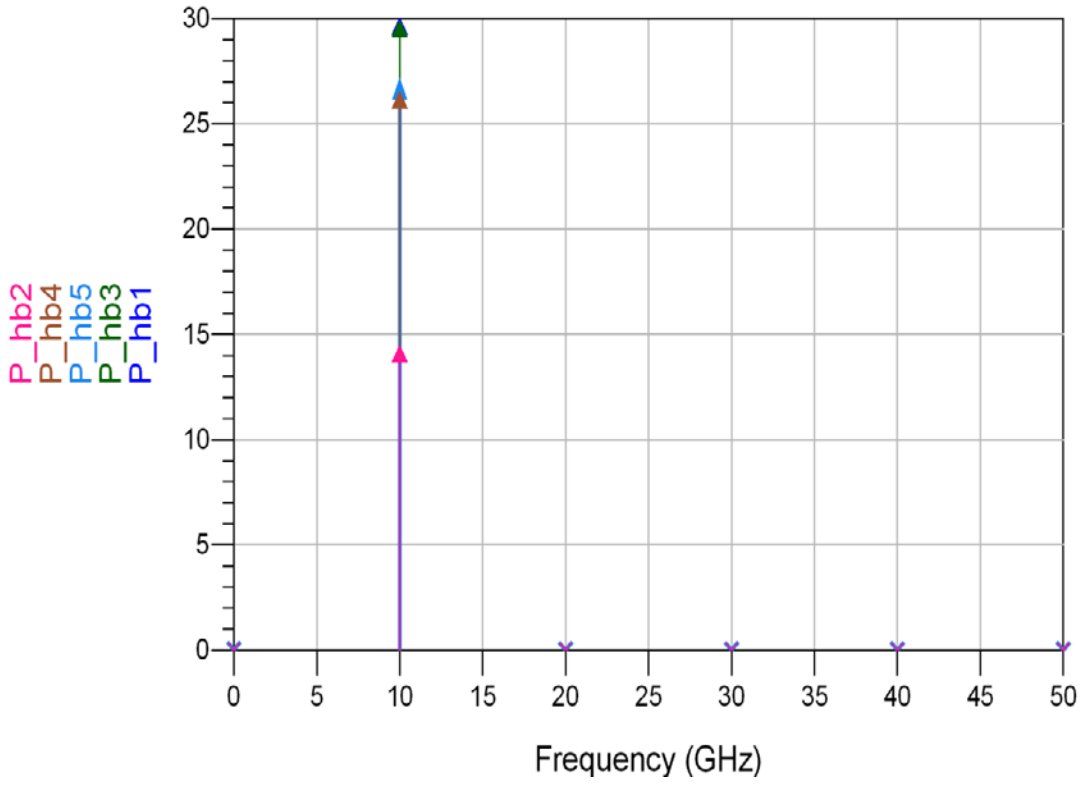

Figure 25. Simulated power spectra at five probe locations for the mismatched circuit.

HB simulated results for matched and mismatched circuits are listed in Table 4.

Table 4. Harmonic balance results for different load circuits at 10 GHz.

Probe	Power measured in matched circuit (dBm)	Power measured in mismatched circuit (dBm)
P_hb1	30	30
P_hb2	≈0	14.437
P_hb3	30	29.878
P_hb4	26.99	26.478
P_hb5	26.99	26.99

4. Summary

For the matched circuit, both transient and harmonic balance simulation results using the time and frequency sources show that power going back to the circulator is negligible compared to the input power. Thus, it can be concluded that there is no power reflection when the circuit is perfectly matched. When connecting different impedances, such as a 100 ohm load at one terminal, the average power reflected toward the source is 0.05556 W divided by two, or 14.437 dBm. The simulated results in ADS verify that the power reflected corresponds to the theoretical results based on the different loads.

C. SYSTEM SIMULATION

Before a comprehensive rectenna system is simulated in ADS, several design parameters are investigated to see their impact on overall performance. One is an optimization of the transmission lines before and after the diodes (Figure 26). By sweeping the length, we observe its effect on the maximum output power and select the best length for the transmission lines. System simulations in both the time and frequency domains are conducted and compared with theoretical results.

1. Transmission Line Optimization

To find the best electrical length for ideal transmission lines, a fixed input power is transmitted and the output power is observed. For a full-wave rectenna, the top transmission lines (TL1 and TL3) and lower transmission lines (TL2 and TL4) are symmetric. So the electrical length parameters for TL1 and TL2 are changed at the same time as shown in Figure 26. They are varied first, and the others remain constant. Then, because TL3 and TL4 are symmetric, those two transmission lines are changed at the same time.

The simulated results are presented in Figure 27 to Figure 29. Probe_1 is the input power and Probe_2 is the output power. To achieve the maximum efficiency, maximum output power is chosen based on fixed input power. Therefore, the optimized electrical lengths are selected based on the maximum output power, illustrated in Figure 27 to Figure 29. These lines are modeled as ideal lossless transmission lines.

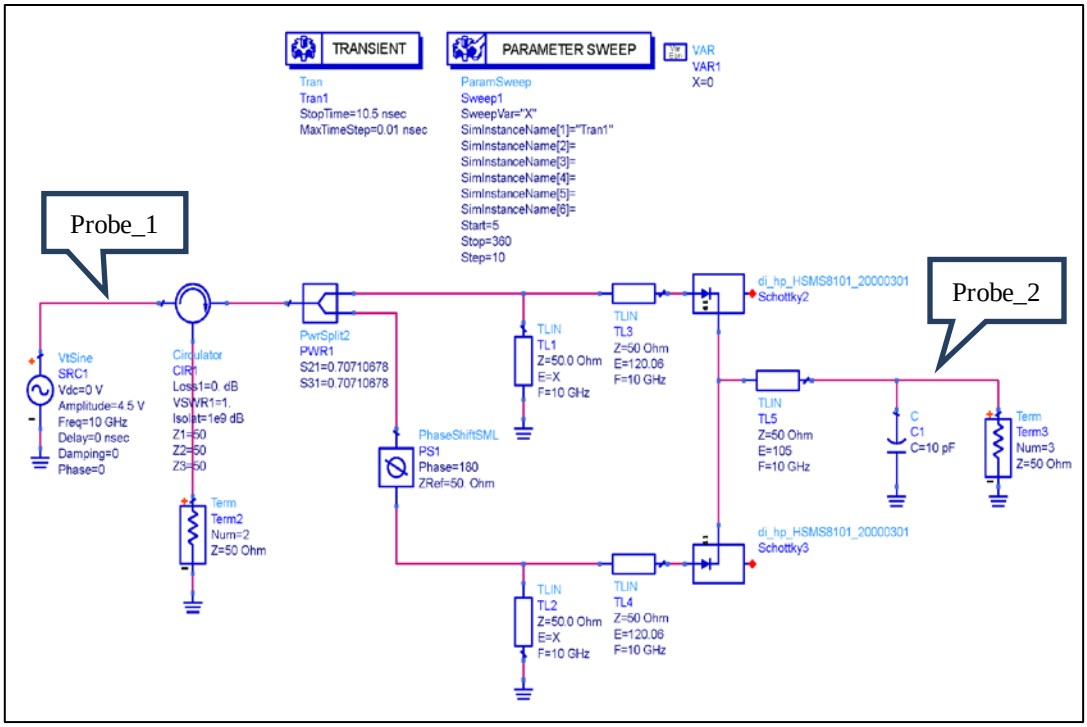

Figure 26. Transmission lines in the post-rectification part of the circuit.

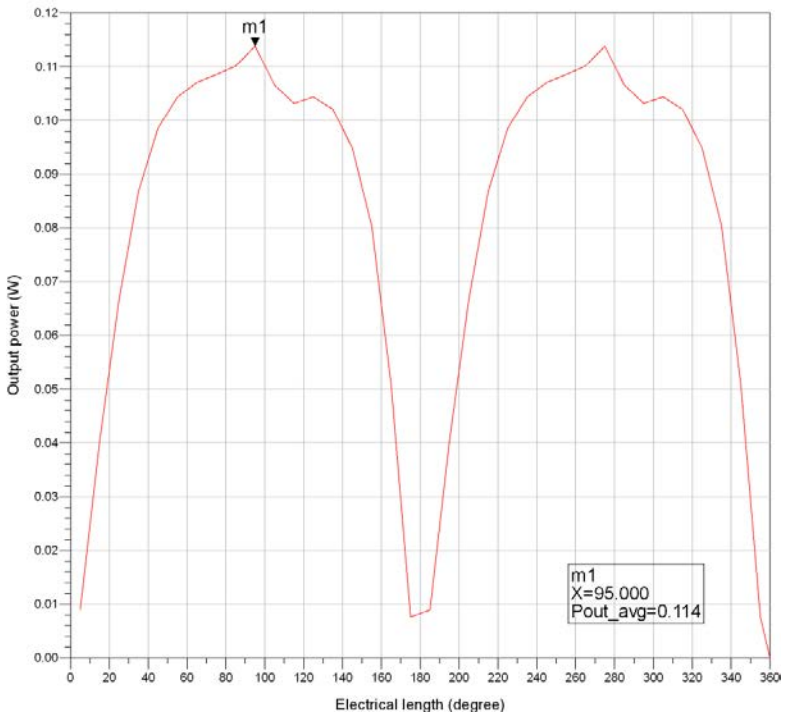

Figure 27. Output power when sweeping electrical length for TL1 and TL2.

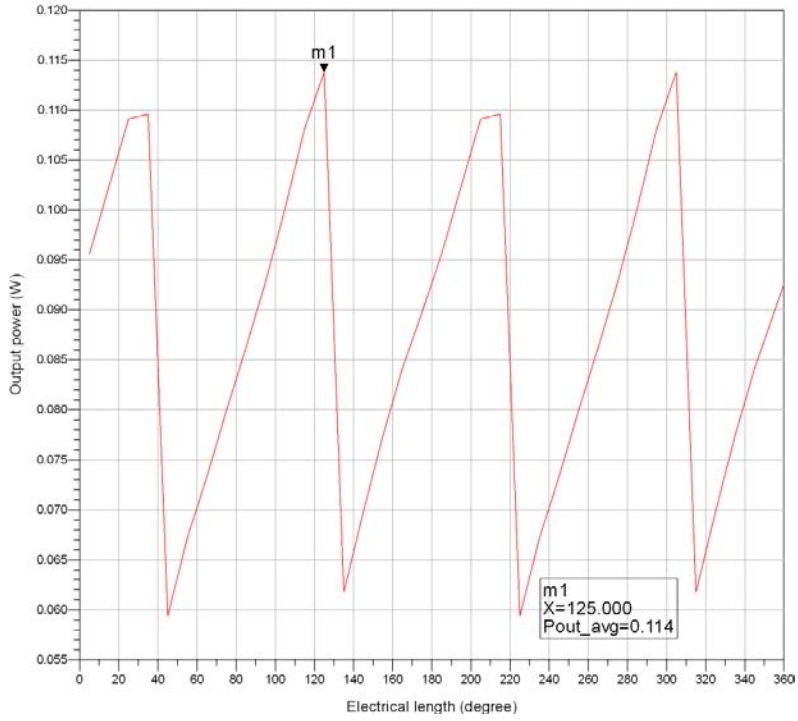

Figure 28. Efficiency when sweeping electrical length for TL3 and TL4.

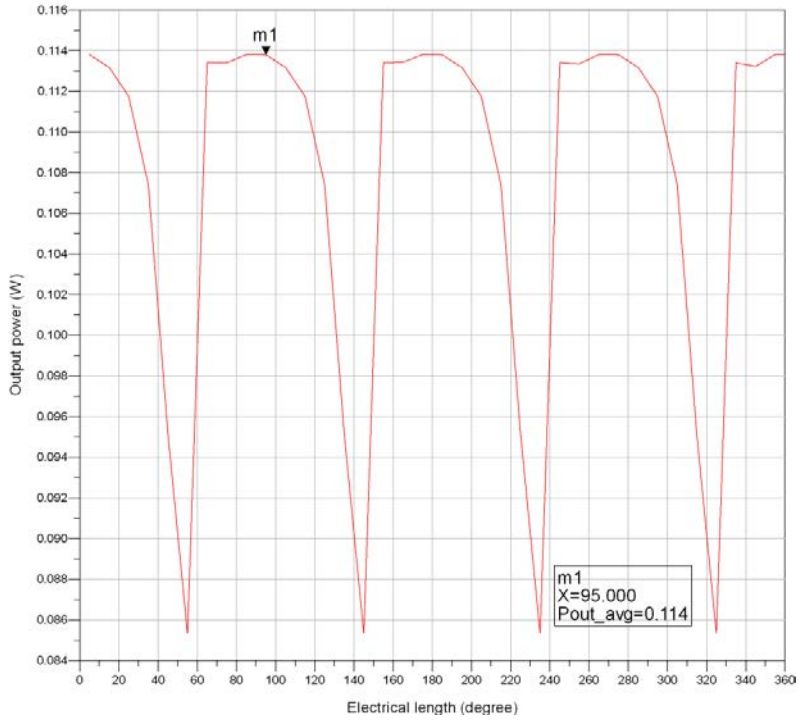

Figure 29. Output power when sweeping electrical length for TL5.

As the hardware is to be tested using Rogers RT/Duroid 5880LZ high-frequency laminate, all the parameters according to [42], such as loss tangent, dielectric constant, and copper cladding are used in ADS as a microstrip material database. For a realistic condition, all ideal transmission lines need to be converted to microstrip transmission lines, so that the simulation can include effects such as losses.

ADS provides a LineCalc tool that can convert parameters between ideal transmission lines and microstrip transmission lines given the microstrip substrate data. Transmission line conversion is achieved as shown in Figure 30 by directly importing microstrip substrate information to LineCalc through the schematic window.

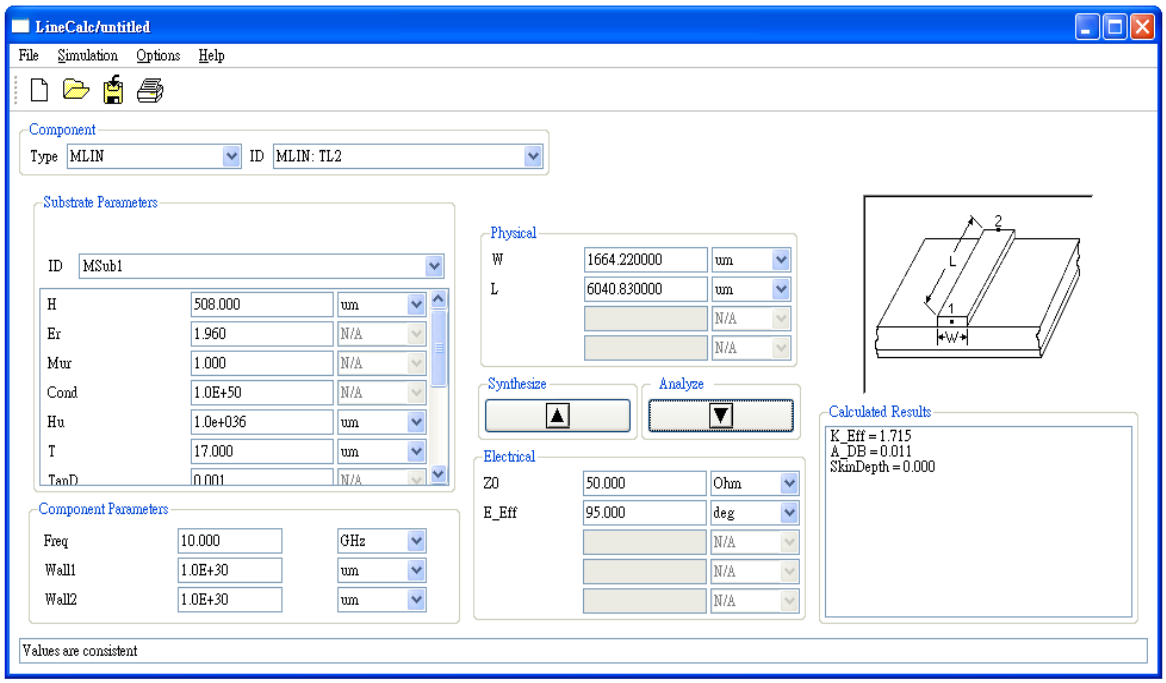

Figure 30. Transmission line calculator in ADS.

To get the optimized value, fine tuning was done for all transmission lines. With the given microstrip material parameters and electrical parameters, the LineCalc tool can calculate physical widths and lengths. The corresponding ideal transmission lines and microstrip transmission lines are listed in Table 5.

Table 5. Parameters for ideal and microstrip transmission lines.

	Ideal		Microstrip	
Transmission line	Impedance (Ohm)	Electrical length (deg)	Physical width (μm)	Physical length (μm)
TL1	50	85	1664.22	5404.95
TL2	50	85	1664.22	5404.95
TL3	50	125	1664.22	7948.46
TL4	50	125	1664.22	7948.46
TL5	50	95	1664.22	6040.83

2. Transient Simulation

When replacing all ideal transmission lines with microstrip lines, the simulation configuration of the rectifier circuit is shown in Figure 31.

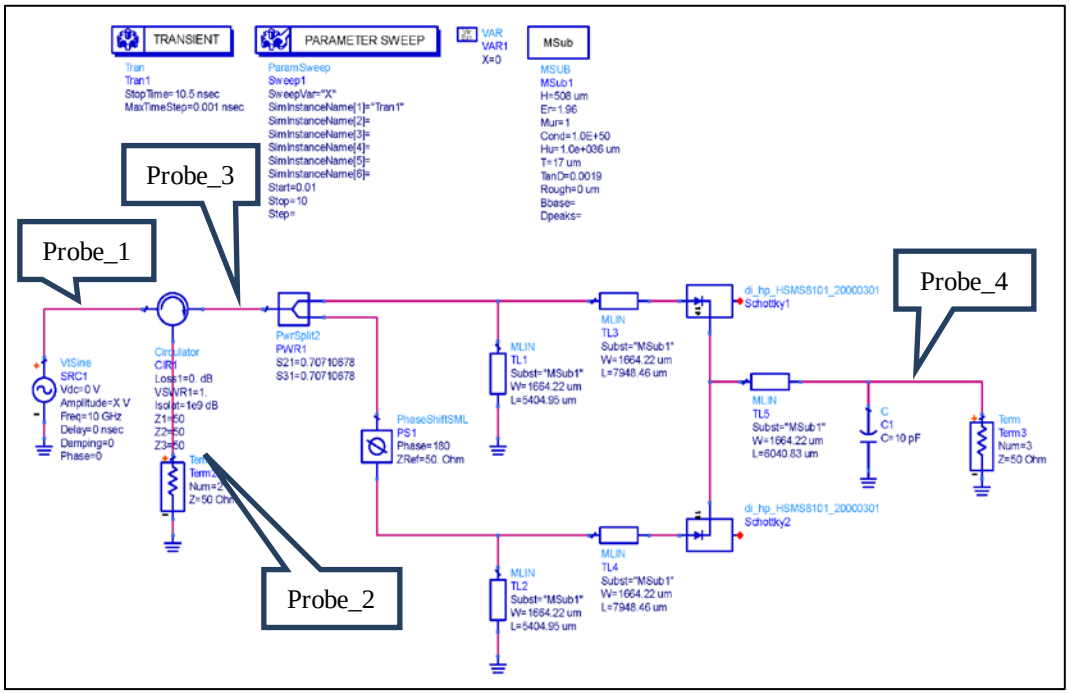

Figure 31. Full-wave rectenna configuration with microstrip lines for the transient simulation.

It can be seen that the output power at Terminal 3, shown in Figure 32, is converted to dc power. Probe_1 is the incident input power, Probe_2 is the power reflected back to the source, Probe_3 is the power transmitted towards the rectifier, and Probe_4 is the output power. The average value of the output power is about 0.11 W, while the input power is 0.2 W.

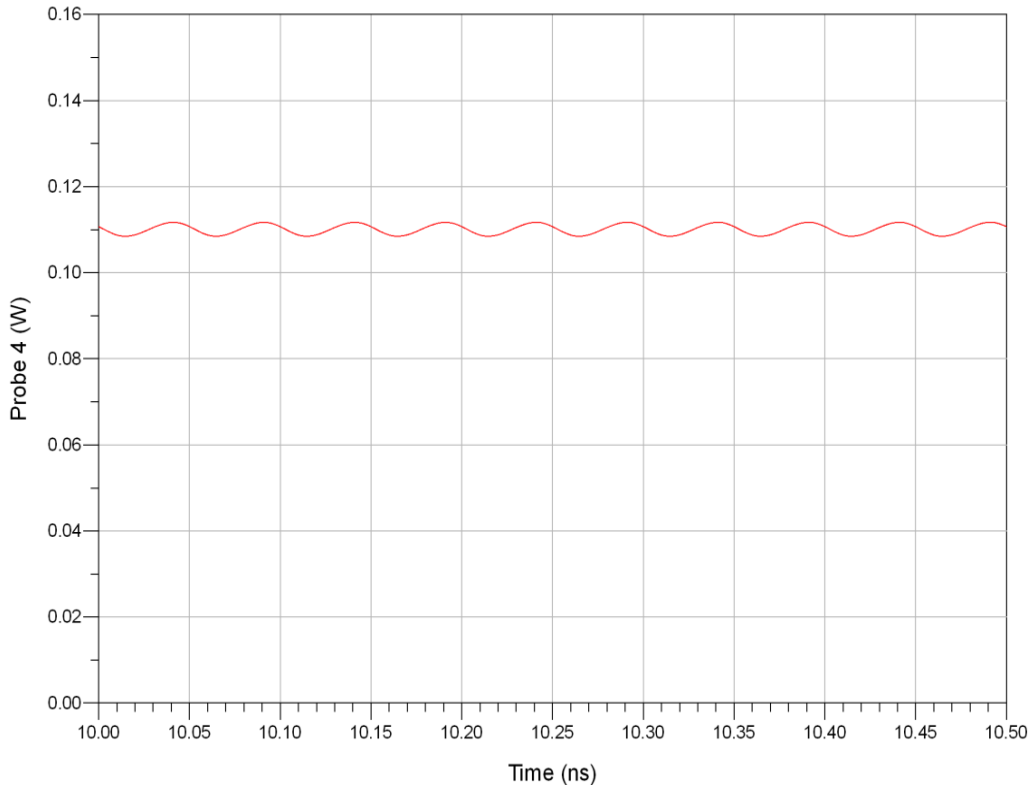

Figure 32. Output power for the full-wave rectenna circuit, transient simulation.

The efficiency plot is illustrated in Figure 33, indicating that the maximum efficiency is 54% when the input power is 0.2 W. For the same input power, the maximum efficiency is about 10% lower than Liu claimed in his thesis. This indicates that not all power is transmitted to load. There is some power loss within the circuit due to microstrip losses and multiple reflections.

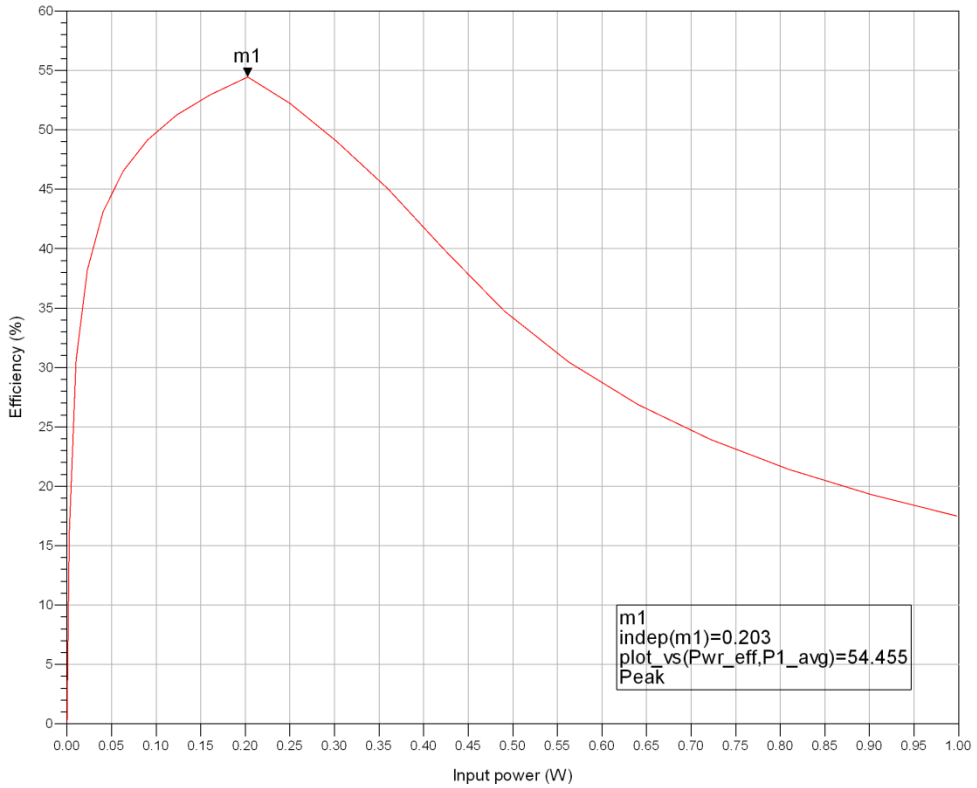

Figure 33. Efficiency plot for optimized full-wave rectenna.

To analyze power reflection within the circuit, the input power is fixed at 0.2 W, where the efficiency is maximum. The average power is calculated at different nodes, and the results are listed in Table 6. With the given incident power of 0.202 W and reflected power of 0.043 W, the reflection coefficient can be obtained from Equation (4.4). Therefore, the reflection coefficient of the rectenna circuit is 0.4614. Since the reflection coefficient is known, the full-wave rectenna impedance can be derived by applying Equation (4.3), which gives 18.4 ohms. For measuring how well the circuit is matched to the load, the return loss (RL) can be found for comparison. A good matched circuit will result in high return loss. Based on reference [41], the return loss is expressed as

$$RL(dB) = -20\log_{10}|\Gamma| \tag{4.6}$$

where Γ is reflection coefficient. The computed return loss is 6.719 dB.

Table 6. Average power at different circuit nodes in the transient simulation.

Probe	Average power (W)
Probe_1	0.202
Probe_2	0.043
Probe_3	0.164
Probe_4	0.110

3. Harmonic Balance Simulation

In order to see the power distribution at different frequencies, a harmonic balance simulation was conducted as shown in Figure 34.

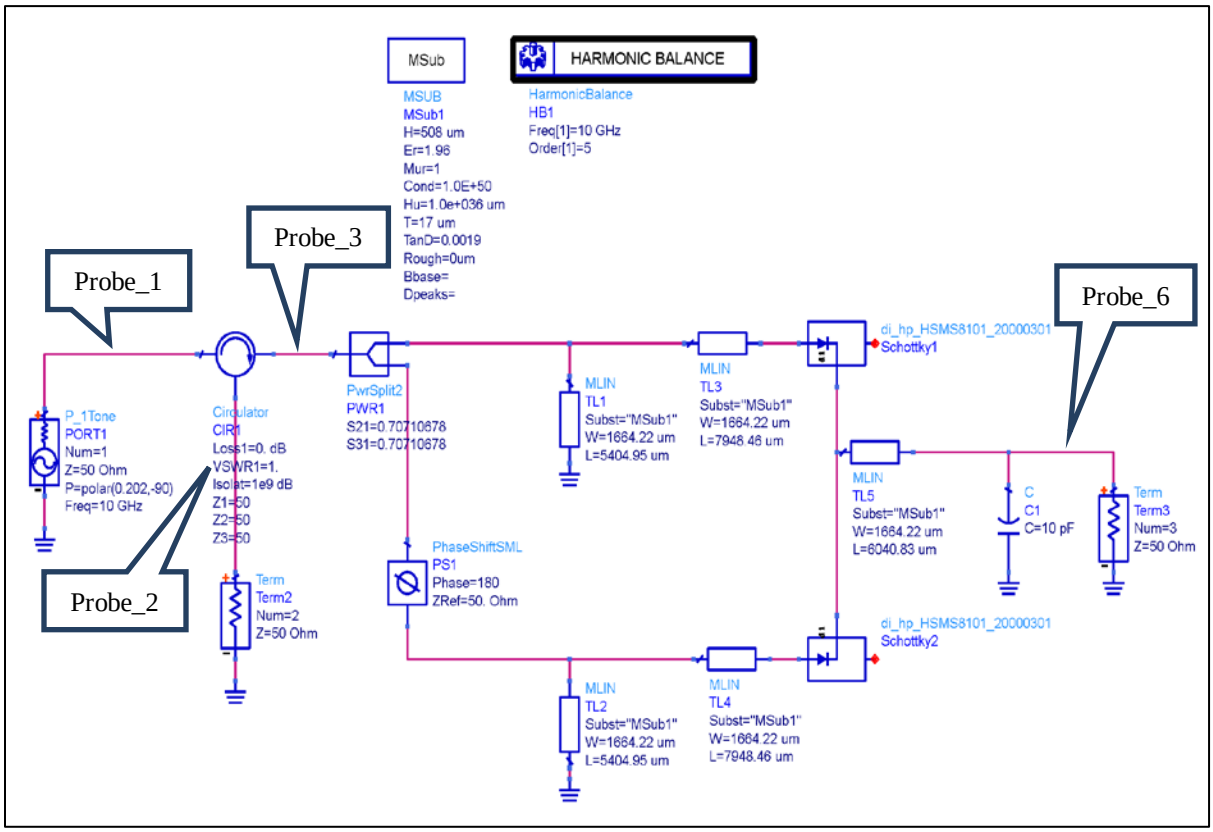

Figure 34. Optimized full-wave rectenna simulation configuration in HB.

Power levels before and after the rectifier circuit are presented in Figure 35. P_hb1 are the input power harmonics, and P_hb6 are the output power harmonics. It can be seen from Figure 35 that most of power is transferred to dc at the output. At the output, it is evident that harmonics at frequency of 10, 30 and 50 GHz are eliminated by the rectifier. There are two harmonics at frequencies of 20 and 40 GHz. Compared with dc, two harmonics can be ignored since they are over 40 dB smaller than the dc signal.

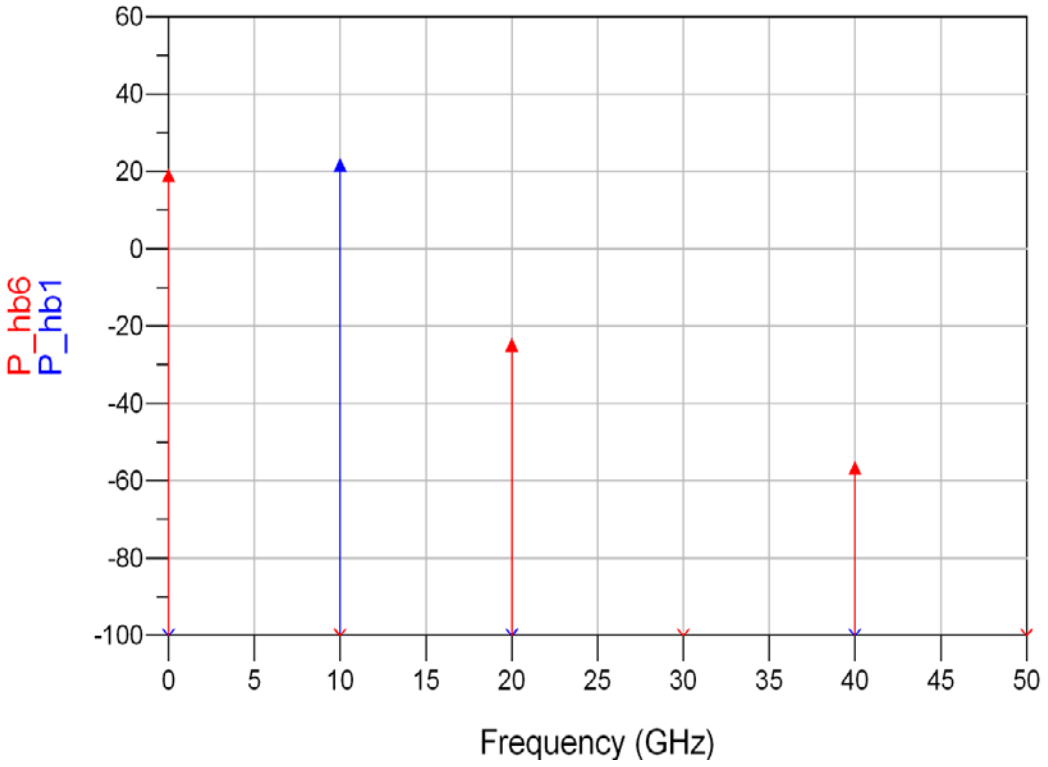

Figure 35. Simulated power spectrum plots.

By summing up power at each frequency, the average power at different nodes was calculated and listed in Table 7. Probe_1 is the incident input power, Probe_2 is the power reflected back to the source, Probe_3 is the power transmitted towards the rectifier, and Probe_6 is the output power.

Table 7. Average power at different nodes in HB simulation.

Probe	Average power (W)
Probe_1	0.202
Probe_2	0.041
Probe_3	0.161
Probe_6	0.109

With the known incident and reflected power, a reflection coefficient can be obtained as 0.4505 using Equation (4.4). From the reflection coefficient, the rectenna circuit impedance is calculated to be 18.9 ohms using Equation (4.3). The return loss can also be estimated using Equation (4.6) to obtain 6.956 dB.

4. Efficiency vs. Frequency

Up to this point, all HB simulations are based on a frequency of 10 GHz. There are different output responses for different frequencies. Thus, efficiency plots at different frequencies were simulated and shown in Figure 36, verifying whether we obtain the maximum output power at a frequency of 10 GHz. Efficiency plots from 8 GHz to 10.5 GHz are presented, illustrating that as frequency is decreased, the optimum point shifts lower. It can also be seen that maximum output power is 0.103 W when the frequency is 10 GHz at an input power of 0.18 W, yielding an efficiency of 57%. The maximum efficiency is 66% when the frequency is 8.5 GHz at an input power of 0.1 W, delivering an output power of 0.066 W.

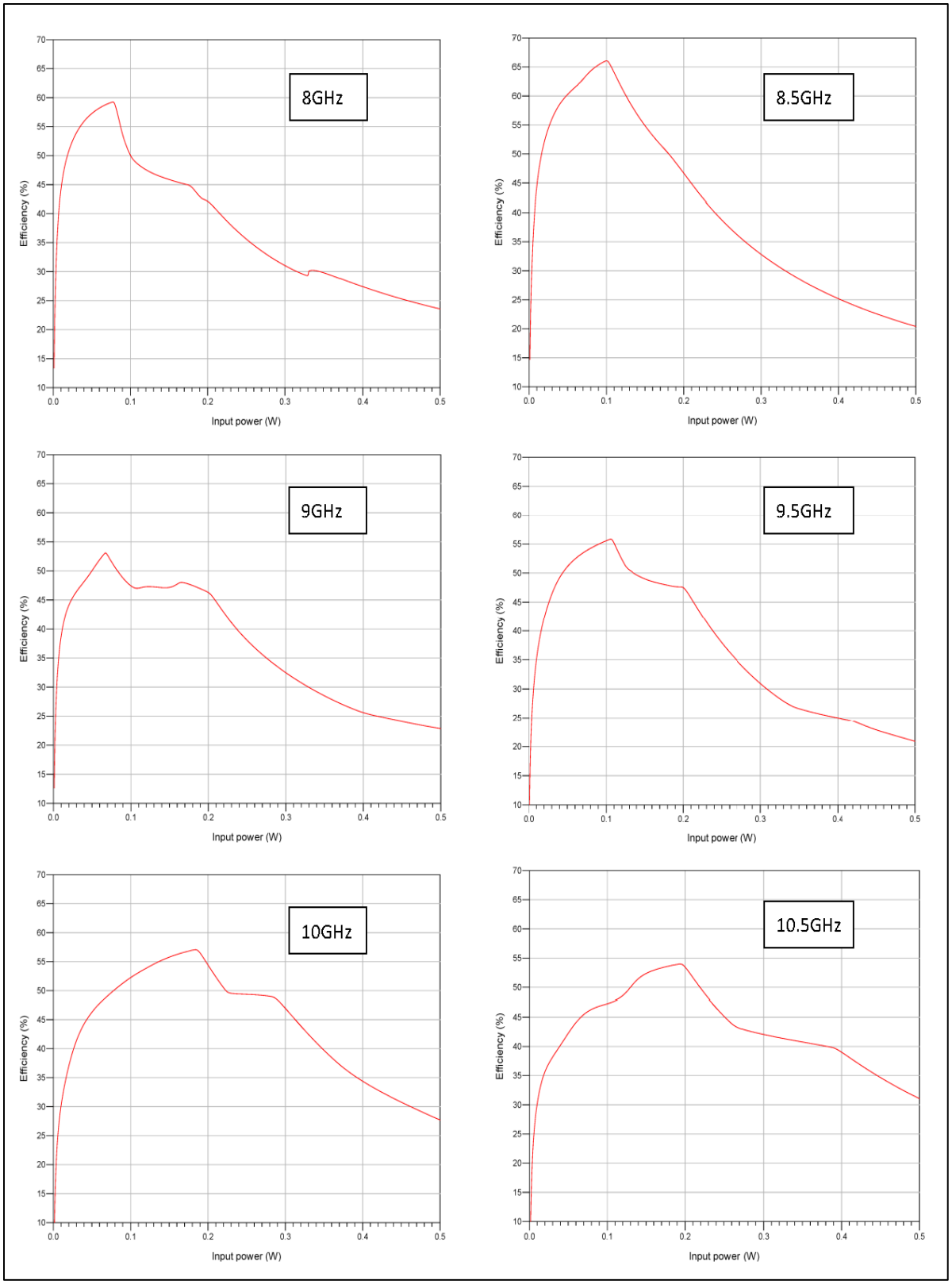

Figure 36. Efficiency plots versus input power for different frequencies.

D. FREE SPACE LINK SIMULATION

In preparation for measurements, the next step is to include the free space power transmission through the atmosphere (Figure 1) using the Friis transmission formula [43]. The total power at the receiving antenna is found by summing up the incident power density over the area of the receiving antenna. The incident power can be converted into available power at the output of the antenna based on several factors, such as antenna type, pointing direction, polarization and so on. The gain of the transmitting antenna can be calculated using

$$G_t = \frac{4\pi}{\lambda^2} A_{et} \tag{4.7}$$

where A_{et} is the effective area of the transmitting antenna. For a transmitting antenna that is not isotropic but has a gain G_t and with a maximum power density in the direction of the receiving antenna, the power density at distance R is

$$S = \frac{P_t G_t}{4\pi R^2}. \tag{4.8}$$

With this power density, the available power at the receiving antenna can be calculated from

$$P_r = SA_{er} = \frac{P_t G_t}{4\pi R^2} A_{er} \tag{4.9}$$

where A_{er} is the effective aperture of the receiving dipole antenna. By applying Equation (4.7), we have the effective aperture of the receiving antenna in terms of antenna gain and wavelength. Therefore, the available power at the receiving antenna output is

$$P_r = \frac{P_t G_t G_r \lambda^2}{(4\pi R)^2}. \tag{4.10}$$

The overall power efficiency is defined as the total dc power measured at the output of the rectifier circuit (P_{dc}) over the time-average input rf power, which is the available power at the output of the receiving antenna (P_r):

$$\eta = \frac{P_{dc}}{P_r}. \tag{4.11}$$

For comparison with measured data in the next chapter, we calculate the received power using the laboratory hardware parameters. For wireless power propagation, the transmitting horn antenna gain is 16.7 dB, the receiving full-wave dipole antenna gain is 6.255 dB, the distance between two antennas is 1 m, and the wavelength is 0.03 m. In order to achieve maximum output power, the input received power should be 0.18 W according to the simulation parameters (Figure 37).

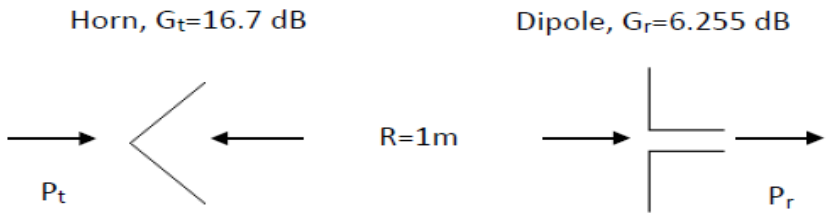

Figure 37. Simulation parameters for antennas.

Therefore, a transmitted power of 160 W is required at a range of 1 m. The available laboratory equipment can only provide 1 W into the transmitting antenna. Assuming an ideal transmission link, we estimate the received power at different frequencies using Equation (4.10), listed in Table 8.

Table 8. Simulated received power at different frequencies, 1 W transmitted power.

Frequency(GHz)	Received power (W)	Frequency(GHz)	Received power (W)
8	1.76×10^{-3}	9.3	1.30×10^{-3}
8.1	1.72×10^{-3}	9.4	1.27×10^{-3}
8.2	1.67×10^{-3}	9.5	1.25×10^{-3}
8.3	1.63×10^{-3}	9.6	1.22×10^{-3}
8.4	1.60×10^{-3}	9.7	1.20×10^{-3}
8.5	1.56×10^{-3}	9.8	1.17×10^{-3}
8.6	1.52×10^{-3}	9.9	1.15×10^{-3}
8.7	1.49×10^{-3}	10.0	1.13×10^{-3}
8.8	1.45×10^{-3}	10.1	1.10×10^{-3}
8.9	1.42×10^{-3}	10.2	1.08×10^{-3}
9.0	1.39×10^{-3}	10.3	1.06×10^{-3}
9.1	1.36×10^{-3}	10.4	1.04×10^{-3}
9.2	1.33×10^{-3}	10.5	1.02×10^{-3}

Using the received power in Table 8 as the input power to the rectifier circuit, we can calculate an estimate of the output dc power and efficiency using Equation (4.11). An efficiency plot versus frequency for a 50 ohm load is shown in Figure 38. It is evident that lower frequencies can achieve higher efficiencies with low input power than higher frequencies. This fact is evident in the plots in Figure 36. The optimized point is no longer at 10 GHz, but shifted to 8.2 GHz.

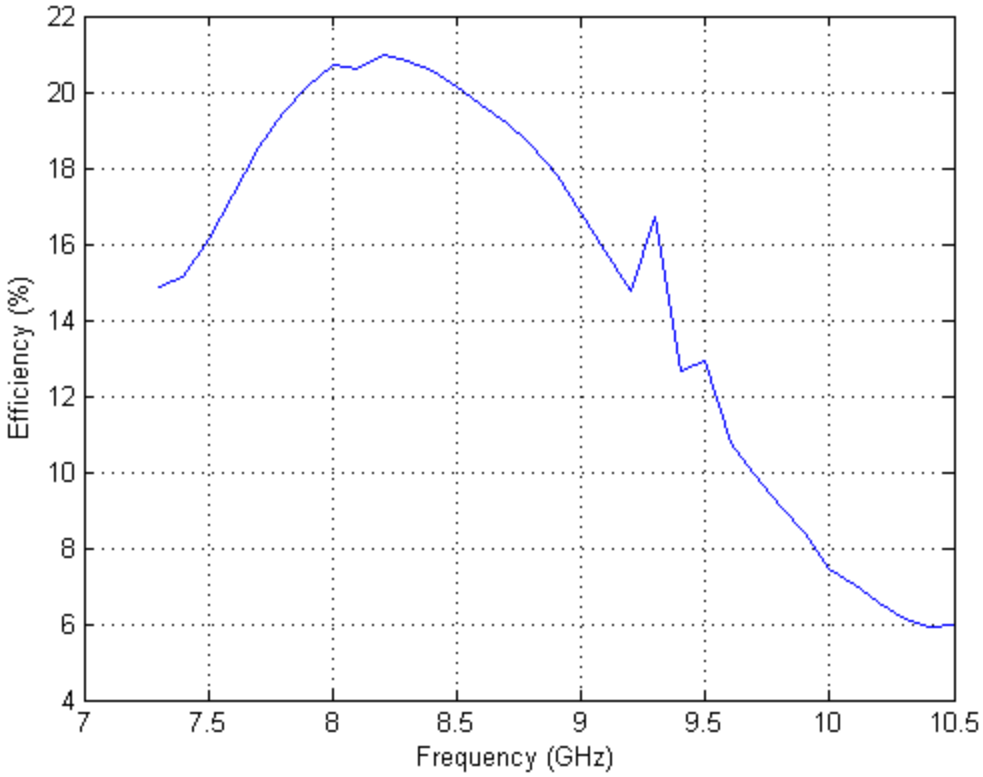

Figure 38. Simulated efficiency curve for different frequencies with 50 ohm load.

E. SUMMARY

In this chapter, the behavior of reflected power and its effect on the full-wave rectenna was investigated in both time and frequency domains. Two simulated results from transient and harmonic balance simulations were very close. With the calculated rectenna circuit impedance of 18 ohm, it is evident that the circuit is not matched with a 50 ohm load, which is the value at which the transmission lines are tuned to optimum.

The maximum efficiency is 54%, which is about 10% lower than Liu claimed with the same input power [8]. This is due to power reflection in the circuit.

The maximum efficiency point and maximum output power were also discussed in this chapter. Maximum efficiency is 66% at a frequency of 8.5 GHz with an input power of 0.1 W, giving a 0.066 W output dc power. The maximum output power can be obtained as 0.103 W at a frequency of 10 GHz with an input power 0.18 W, giving an efficiency of 57%. It was demonstrated that for low input power levels, the efficiency peak moves to lower frequencies.

Hardware experiments and comparison with simulation results are discussed in the next chapter.

V. HARDWARE TESTING

In this chapter, the design, fabrication and testing of the rectenna is described. The fabricated hardware was tested in the NPS Microwave Laboratory.

A. ANTENNA ELEMENT

A full-wave dipole rectenna was designed using Computer Simulation Technology (CST) Microwave Studio (MWS) software. CST can be used for the design of microwave circuits and antennas. The rectenna element is a dipole. The design was explained by Liu [8]. The dipole and feed lines can be seen in Figure 39.

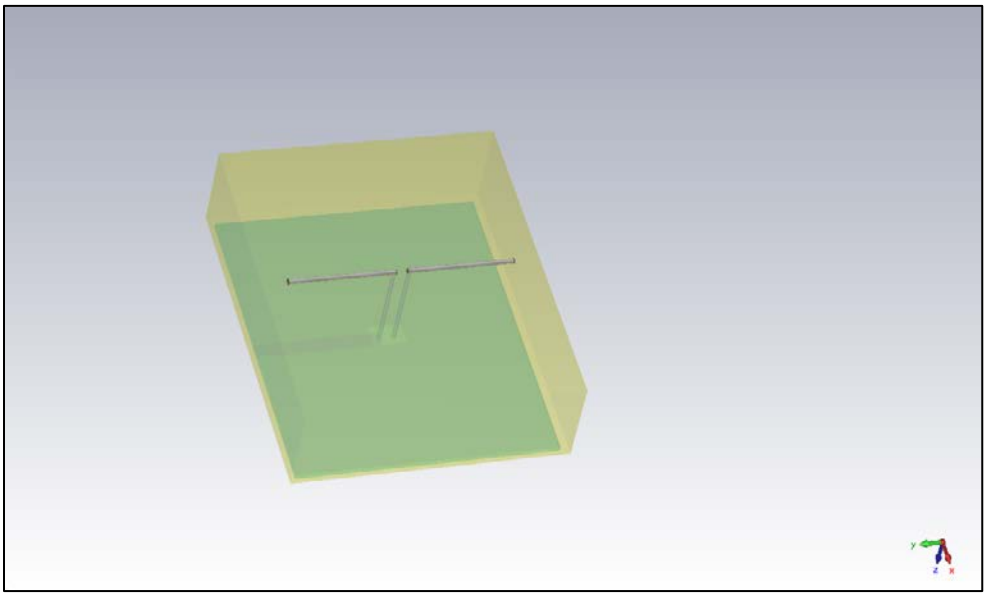

Figure 39. Dipole antenna model in CST MWS.

For the purpose of measuring S-parameters, the feed line is attached to a 50 ohm microstrip line. The S-parameter plot is illustrated in Figure 40. From Figure 40, it is obvious that the minimum S_{11} value is at 9.1 GHz. This means the optimized frequency for the antenna is shifted to 9.1 GHz due to the feed lines and the small ground plane.

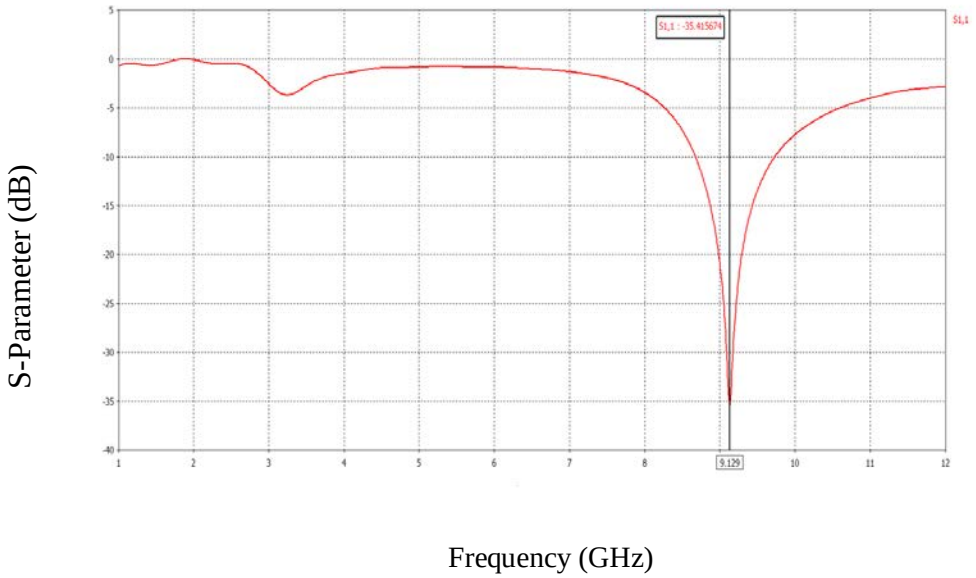

Figure 40. Full-wave dipole antenna frequency response (length 30 mm).

Since the desired frequency of operation is 10 GHz, the length and height are tuned. The dipole length was adjusted for the best performance, and it is found to occur at a length of 25 mm at 10 GHz, as shown in Figure 41. The S_{11} value is about -21.2 dB. Therefore, dipole length is selected as 25 mm.

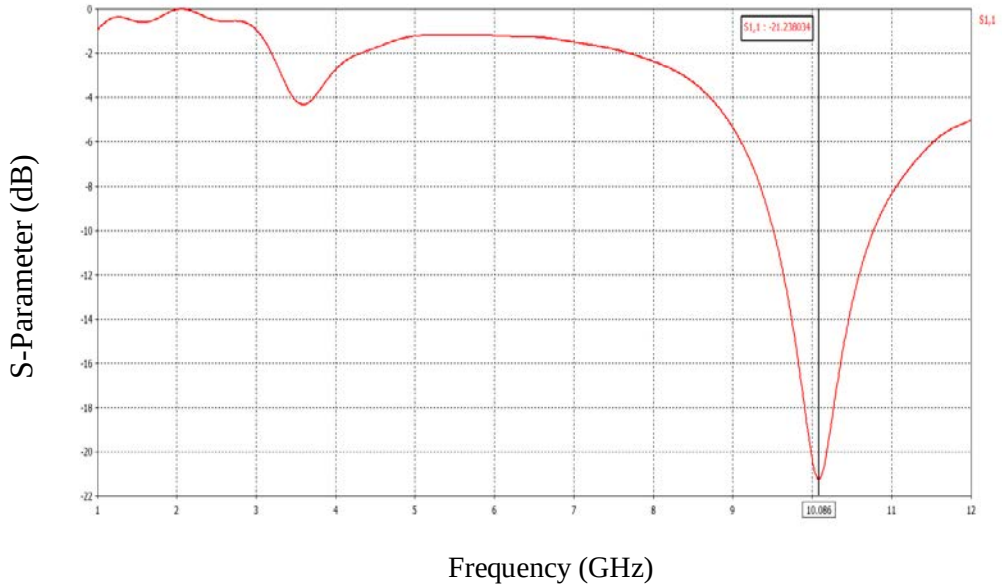

Figure 41. Dipole antenna frequency response (length 25 mm).

B. RECTIFIER STRUCTURE

1. Dielectric Materials

Based on a Rogers Corporation datasheet [42], the dielectric material used in the rectifier (Rogers RT/Duroid 5880LZ high-frequency laminate) has specifications listed in Table 9.

Table 9. Dielectric materials for Rogers RT/Duroid 5880LZ (After [42]).

Dielectric Constant (ε_r)	1.96 ∓ 0.04
Dissipation Factor ($\tan\delta$)	Typ: 0.0019 (10 GHz/ 23°C) Max: 0.0027
Standard Thickness (h)	0.020" (0.508 mm) $\pm$ 001
Standard Copper Cladding	1/2 oz (17 μm)

2. Layout

The rectifier circuit is based on the ADS model shown in Figure 31. The HSMS 8101 Sckottky diode was soldered onto the printed circuit board. The material used for ground plane is 0.5 ounce copper, and the cutout area for the dipole antenna at the center is 5.25 mm by 2.6 mm, as shown in Figure 42. There are three shorting pins with diameter of 0.5 mm connecting the microstrip line to ground.

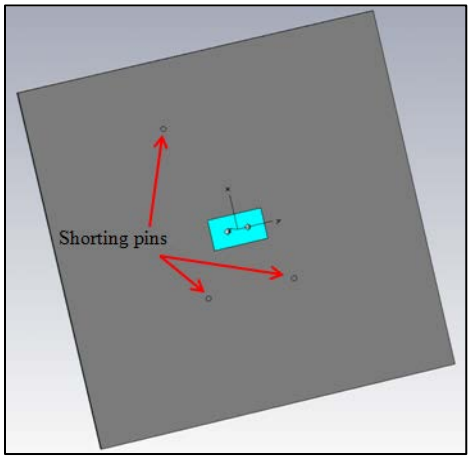

Figure 42. Ground plane layout in CST model.

The front side of the circuit is shown in Figure 43. The impedance matching unit was bent in order to have a compact design and minimize the weight. The assembled rectenna hardware is shown in Figure 44. The weight of the rectenna, including foundation support used to fix the dipole antenna onto the printed circuit board, is approximately 5 grams, and the area of the rectenna is 35 mm by 35 mm.

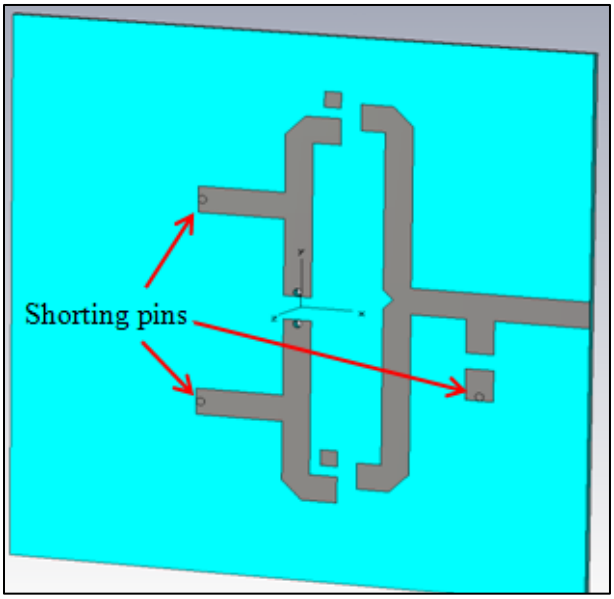

Figure 43. Microstrip panel layout in CST.

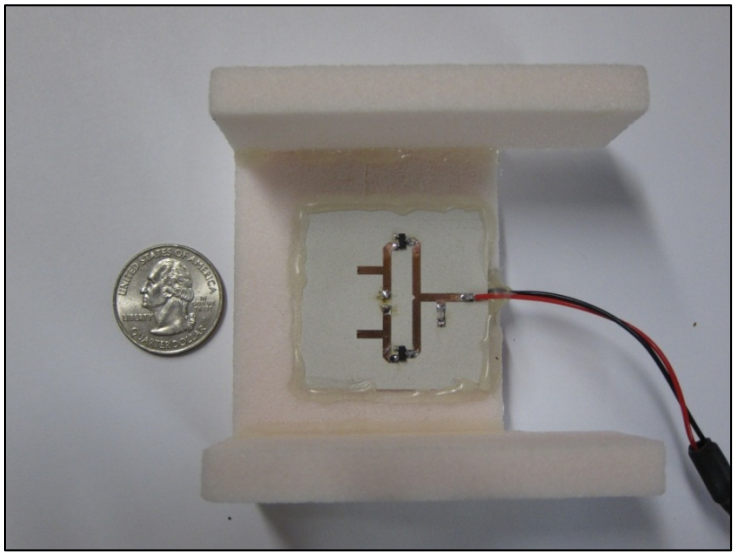

Figure 44. Assembled full-wave rectenna hardware shown a with U.S. coin (quarter).

C. MEASURED PERFORMANCE OF THE RECTENNA

A block diagram of the test configuration is shown in Figure 45. It is basically a free space link. An HP 8341B synthesized sweeper signal generator produces a high frequency sinusoidal signal. This output signal was amplified to 1 W using an Agilent 83020A microwave system amplifier. A horn antenna of area 91.3 mm by 73.9 mm was used for the transmitting antenna with transmitting gain of 16.7 dB. The rectenna hardware was placed at a distance of 1 m in front of the horn antenna. In order to observe the frequency response for comparison with simulated results, frequencies from 8 GHz to 10.5 GHz were tested. On the rectenna side, the load was selected as 51 ohms and connected with rectenna circuit for measuring the dc voltage and current through a voltmeter and ammeter. A photo of the hardware test configuration is shown in Figure 46.

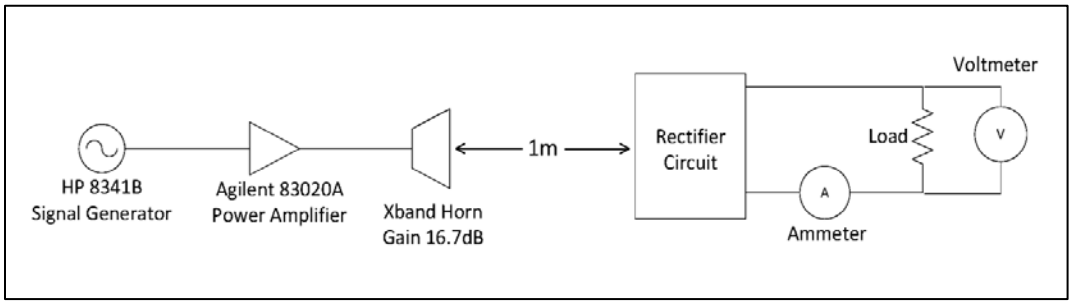

Figure 45. Rectenna hardware testing diagram.

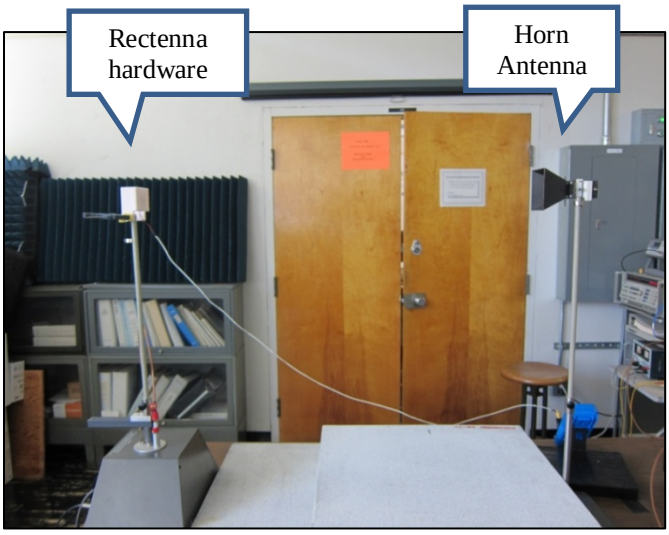

Figure 46. Hardware test setup in the microwave laboratory.

The voltage and current across the 51-ohm load were measured and are listed in Table 10. It can be seen that maximum occurs at the frequency of 8.7 GHz. Therefore, the maximum output power can be calculated simply by multiplication of the voltage and current shown in Table 10.

Table 10. Measured voltage and current across 51-ohm load.

Frequency (GHz)	Voltage (mV)	Current (mA)	Output dc power (W)
8	120.00	2.00	2.400×10^{-4}
8.1	131.90	2.25	2.968×10^{-4}
8.2	146.45	2.54	3.720×10^{-4}
8.3	162.30	2.84	4.609×10^{-4}
8.4	172.43	2.97	5.121×10^{-4}
8.5	180.90	3.16	5.716×10^{-4}
8.6	185.63	3.21	5.959×10^{-4}
8.7	191.24	3.29	6.292×10^{-4}
8.8	173.35	3.03	5.253×10^{-4}
8.9	162.38	2.88	4.677×10^{-4}
9.0	149.44	2.64	3.945×10^{-4}
9.1	146.36	2.56	3.747×10^{-4}
9.2	123.24	2.16	2.662×10^{-4}
9.3	117.80	2.08	2.450×10^{-4}
9.4	102.21	1.81	1.850×10^{-4}
9.5	94.90	1.71	1.623×10^{-4}
9.6	70.62	1.26	8.898×10^{-5}
9.7	69.55	1.24	8.624×10^{-5}
9.8	50.85	0.87	4.424×10^{-5}
9.9	52.17	0.92	4.800×10^{-5}
10.0	29.94	0.56	1.677×10^{-5}
10.1	43.11	0.75	3.233×10^{-5}
10.2	26.64	0.47	1.252×10^{-5}
10.3	31.12	0.56	1.743×10^{-5}
10.4	28.83	0.51	1.470×10^{-5}
10.5	24.54	0.43	1.055×10^{-5}

From the measured output dc power, an efficiency can be calculated using Equation (4.11). The measured efficiency curve is shown in Figure 47. The peak point is at 8.7 GHz instead of 10 GHz as expected for the low transmitted power of 1 W.

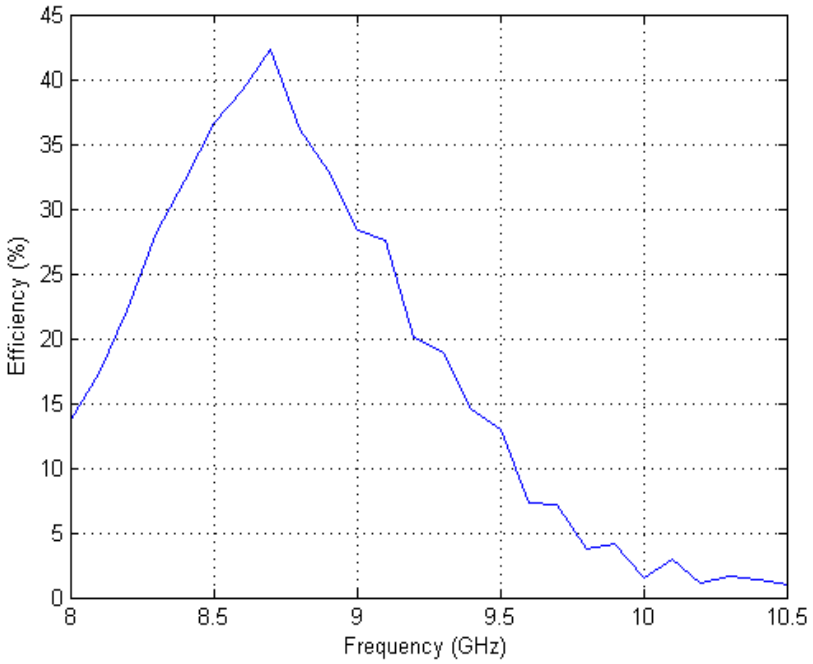

Figure 47. Measured efficiency curve for different frequencies with 51 ohm load.

D. DISCUSSION AND SUMMARY

Based on experimental results, it can be seen that the rectenna has an optimized efficiency when the frequency is 8.7 GHz. It is capable of producing voltages from 25 mV to 191 mV and currents from 0.43 mA to 3.29 mA using the full-wave rectenna and a transmitted power of 1 W. Note that the power limitation of the lab equipment does not allow measurements near the peak of the efficiency curve in Figure 33.

Comparing the efficiency curves in Figure 47 and Figure 37, we see that the measured efficiency is larger than the simulated efficiency in the frequency range of 8.5 GHz to 9 GHz and is smaller than the simulated efficiency when the frequency is above 9.5 GHz. However, the shape and structure of the two curves are very close. The received power is calculated based on the Friis transmission equation, Equation (4.10), and an

ideal microwave link is assumed. At a frequency of 10 GHz, the measured efficiency is about 1.5%, whereas the simulated result is 7.5% for the same input received power. The simulated efficiency is five times greater than the measured efficiency. Thus, there is a loss factor of about five at 10 GHz between measurement and simulation.

There are several possible reasons for the difference between the measured and simulated results.

First, an ideal free space link was assumed in the calculation of efficiency for the measurement. However, for the short range, the rectenna is barely in the transmitting antenna's far-field, so peak transmitting antenna gain may not be realized. Also, there are mismatch losses at various points in the link.

Second, the variation in antenna impedance with frequency is not included in the ADS simulations. It can be seen from Figure 41 that the antenna mismatch changes rapidly with frequency, and this is likely the reason for the steep drop in the measured efficiency between 8–8.5 GHz in Figure 47.

Finally, there may be a mismatch in the frequency bandwidths of the dipole and rectifier circuit. The two parts of the rectenna were optimized for operation at 10 GHz using MWS and ADS. An accurate simulation of the combined circuit could not be done in either tool. It is known that, in some cases, a discrete port in MWS gives scattering parameters that are shifted in frequency [44]. If this occurred, then the overall efficiency curve would be shifted.

In the next chapter, the simulation and test results are summarized. Some conclusions and recommendations for future work are presented.

VI. SUMMARY, CONCLUSIONS AND RECOMMENDATIONS

A. SUMMARY

The performance of a full-wave rectenna design proposed by Liu [8] was simulated and measured, and power reflection and circuit optimization were discussed to make necessary modification for the circuit. Several simulations using ADS and CST were conducted to characterize the behavior of the full-wave rectenna system and optimize the efficiency for 200 mW input power at 10 GHz with a 50 ohm load at the output.

A technique employed in the study was to add a circulator to isolate power reflection in the circuit. Also, a new method of feeding the rectifier with an unbalanced source was investigated to replace the original design. Originally, the voltage source's positive and negative terminals each drove a branch of the full-wave rectifier. The efficiency plot using unbalanced source was evaluated and simulated and found to give similar results as the original bipolar feed. The new feed approach can be applied to the design of new test fixture that directly excites the rectifier. Power reflection tests were run by connecting matched and mismatched impedances to the outputs of the circuits. The results were verified with theoretical values in both the time and frequency simulations.

Another set of simulations addressed the tuning of electrical parameters of the transmission lines before and after the diodes. While sweeping the electrical lengths, the output power was observed so that the best electrical length with maximum output power could be identified. The ideal transmission lines in the simulation were converted to more realistic microstrip transmission lines using the LineCalc Tool that use the actual microstrip dimensions and substrate parameters.

The final optimized circuit was modeled in both transient and harmonic balance simulations. The maximum efficiency is 54% when the input power is 0.2 W, and the estimated return loss is about 7 dB. To verify that the maximum output power occurred at 10 GHz, an efficiency response was conducted at different frequencies shown in Figure

36. At 10 GHz, the maximum output power of 0.103 W is obtained when the input power is 0.18 W, resulting in an efficiency of 57%. Further investigation demonstrated that, as the input power falls below 200 mW, the peak of the efficiency curve shifts lower in frequency.

Based on the ADS rectifier design and the CST dipole design, a prototype rectenna element was fabricated and tested using a free space link. The final length of the dipole was 25 mm. Due to limitations of the laboratory hardware, the transmitted power was 1 W at the horn antenna. Thus, the low received power at the rectenna means that it was operating on the low part of the efficiency curve. Because of the low input power, the peak efficiency shifted to 8.5 GHz, which was also observed in the simulation results.

B. CONCLUSION

Using diode data available from the manufacturer, we optimized a full-wave rectenna for input power around 200 mW at 10 GHz with a 50 ohm load. Efficiencies of 55 to 66 percent were predicted for various circuit designs. However, with microstrip lines, the maximum output power can be achieved when the frequency is 10 GHz with input power of 0.18 W and has a conversion efficiency of 57%. The measured efficiency curve, while similar in shape, was shifted lower in frequency because of the low input power. In order to get an accurate measurement of efficiency, higher input power is needed, but this cannot be obtained using a free space link with the existing amplifier. Therefore, a direct power input to the rectifier circuit that bypasses the dipole must be used.

C. RECOMMENDATIONS

The results of this thesis show the correspondence between measurement and simulation. However, the input power is too small to operate at the peak of the efficiency curve. The reason this power level (200 mW) was chosen is because two prototypes of MAV with different motors could possibly be powered by this output if several rectennas are combined.

Some recommendations are listed next.

1. High Power Efficiency Test

The current simulation is based on a balanced source that accurately represents the dipole antenna. Simulations in Chapter IV showed that a single unbalanced source gives the same result as a balanced source. The hardware can be built with a coaxial input, unbalanced source feeding the two branches of microstrip line with a power splitter. By feeding a power source into the circuit without a dipole antenna, the free space loss is not suffered and higher power is fed directly to the rectifier.

2. Reducing Printed Circuit Board Board Size and Weight

The microstrip line for the current design covers only 80% of the printed circuit board (PCB) surface area. The dipoles could be packed more densely and the circuit area reduced to lighten its weight.

3. Designing Full-Wave Rectenna Array

The current rectenna maximum output power of 0.103 W is not large enough to power most current MAV models. To increase received power, an array can be designed for increasing the power output with a fixed transmitted power.

4. High Directivity Antenna

The gain for the current transmitter horn antenna is 16.7 dB. Higher received power can be achieved if we can use a narrowbeam antenna. Then, most transmitted power will be directed to the receiver dipole antenna. However, the range must be adjusted so that far-field conditions are satisfied. If not, the full transmit antenna gain may not be realized.

THIS PAGE INTENTIONALLY LEFT BLANK

LIST OF REFERENCES

[1] N. Shinohara, Y. Miyata, T. Mitani, N. Niwa, K. Takagi, K. Hamamoto, S. Ujigawa, Jing-Ping Ao and Y. Ohno, "New application of microwave power transmission for wireless power distribution system in buildings," in *Microwave Conference*, pp. 1–4, 2008.

[2] S. Mohrehkesh and T. Nadeem, "Toward a wireless charging for battery electric vehicles at traffic intersections," *14th International IEEE Conference* in *Intelligent Transportation Systems (ITSC)*, pp. 113–118, 2011.

[3] Zou Yuwei, Huang Xueliang, Tan Linlin, Bai Yang and Zhang Jianhua, "Current research situation and developing tendency about wireless power transmission," in *International Conference on Electrical and Control Engineering (ICECE), p*p. 3507–3511, 2010.

[4] T. Yamamoto, K. Fujimori, M. Sanagi and S. Nogi, "The design of mw-class RF-DC conversion circuit using the full-wave rectification," in *Microwave Conference*, pp. 905–908, 2007.

[5] Jae Shin Kim, Wenhsing Wu, Jenshan Lin, A. Verma, Soohwan Jang, F. Ren, S. Pearton, R. Fitch and J. Gillespie, "High-efficiency GaN/AlGaN HEMT oscillator operating at L-band," in *Microwave Conference*, pp. 631–634, 2006.

[6] G. Tsolis, "Theoretical and experimental study of micro air vehicle powered by RF signal at 10 GHz," Master's thesis, Naval Postgraduate School, 2003.

[7] W. C. Brown, "Experiments Involving a Microwave Beam to Power and Position a Helicopter," *IEEE Trans. Aerospace and Electronic Systems*, vol. AES-5, pp. 692–702, 1969.

[8] C. Liu, "An improved rectenna for wireless power transmission for unmanned air vehicles," Master's thesis, Naval Postgraduate School, 2011.

[9] R. McCormmach, *Hertz, Heinrich Rudolf in Dictionary of Scientific Biography*. New York: Scribner, 1976.

[10] John J. O'Neill, *Prodigal Genius: The Life of Nikola Tesla.* New York: Washburn, 1944.

[11] Margaret Cheney, *Tesla: Man Out of Time.* Mattituck, New York: Amereon House, 1981.

[12] A. S. Marincic, “Nikola Tesla and the Wireless Transmission of Energy,” *IEEE Trans. on Power Apparatus and Systems*, vol. PAS-101, pp. 4064–4068, 1982.

[13] W. C. Brown, “The History of Power Transmission by Radio Waves,” *IEEE Transactions on Microwave Theory and Techniques*, vol. 32, pp. 1230–1242, 1984.

[14] W. C. Brown, “A Survey of the Elements of Power Transmission by Microwave Beam,” vol. 9, pp. 93–105, 1961.

[15] P. E. Glaser, “Power from the sun - its future.” *Science, New Series*, vol. 162, No. 3856 (Nov. 22, 1968), pp. 857–861, 1968.

[16] W. C. Brown, “The Solar Power Satellite as a Source of Base Load Electrical Power,” *IEEE Transactions on Power Apparatus and Systems*, vol. PAS-100, pp. 2766–2774, 1981.

[17] S. Sasaki and K. Tanaka, “Wireless power transmission technologies for solar power satellite,” in *Microwave Workshop Series on Innovative Wireless Power Transmission: Technologies, Systems, and Applications (IMWS)*, pp. 3–6, 2011.

[18] P. E. Glaser, O. E. Maynard, J. J. R. MACKOVCIAK and E. I. Ralph. Feasibility study of a satellite solar power station [final report], Washington: NASA. 1974.

[19] R. M. Dickinson, “Performance of a high-power, 2.388-GHz receiving array in wireless power transmission over 1.54 km,” in *Microwave Symposium*, pp. 139–141, 1976.

[20] U.S. Office of Technology Assessment, *Solar Power Satellites.* 1981.

[21] J. C. Mankins, “A fresh look at space solar power,” in *Energy Conversion Engineering Conference*, vol. 1, pp. 451–456, 1996.

[22] M. Lifsher, “A giant leap toward space-based solar power,” *Los Angeles Times*, May 17, 2009. http://articles.latimes.com/2009/may/17/business/fi-space-solar17

[23] N. Shinohara and S. Kawasaki, “Recent wireless power transmission technologies in japan for space solar power station/satellite,” in *Radio and Wireless Symposium*, pp. 13–15, 2009.

[24] S. Sasaki, K. Tanaka, K. Higuchi, N. Okuizumi, S. Kawasaki, N. Shinohara, K. Senda, and K. Ishimura, “A new concept of solar power satellite: Tethered-SPS,” in *Acta Astronautica*, pp. 153–165, 2006.

[25] W. C. Brown, “Electronic and mechanical improvment of the receiving terminal of a free space microwave power transmission system,” Raytheon Company, Wayland, MA, Tech. Rep. PT-4964, NASA Rep. CR-135194, 1977.

[26] W. C. Brown and J. F. Triner, “Experimental thin-film, etched-circuit rectenna,” in *Microwave Symposium Digest*, pp. 185–187, 1982.

[27] W. C. Brown, “Performance characteristics of the thin-film, etched-circuit rectenna,” in Microwave Symposium Digest, pp. 365–367, 1984.

[28] R. J. Gutmann and J. M. Borrego, “Power combining in an array of microwave power rectifiers” *IEEE Trans. Microwave Theory and Techniques*, vol. 27, no. 12, pp. 958–968, 1979.

[29] N. Shinohara and H. Matsumoto, “Dependence of dc output of a rectenna array on the method of interconnection of its array elements,” *Electr. Eng. Jpn.* , vol. 125, no. 1, pp. 9–17. 1998.

[30] T. Yoo and K. Chang, “Theoretical and experimental development of 10 and 35 GHz rectennas,” *IEEE Trans. Microwave Theory and Techniques*, vol. 40, no. 6, pp. 1259–1266, 1992.

[31] S. S. Bharj, R. Camisa, S. Grober, F. Wozniak and E. Pendleton, “High efficiency C-band 1000 element rectenna array for microwave powered applications,” in *Microwave Symposium Digest*, vol. 1, pp. 301–303, 1992.

[32] J. O. McSpadden, Lu Fan and Kai Chang, “Design and experiments of a high-conversion-efficiency 5.8-GHz rectenna,” *IEEE Trans. Microwave Theory and Techniques*, vol. 46, no. 12, pp. 2053–2060, 1998.

[33] J. O. McSpadden and K. Chang, “A dual polarized circular patch rectifying antenna at 2.45 GHz for microwave power conversion and detection” in *Microwave Symposium Digest*, vol. 3, pp. 1749–1752, 1994.

[34] Young-Ho Suh and Kai Chang, “A high-efficiency dual-frequency rectenna for 2.45- and 5.8-GHz wireless power transmission,” *IEEE Trans. Microwave Theory and Techniques*, vol. 50, no. 7, pp. 1784–1789, 2002.

[35] D. H. Werner and S. Ganguly. “An overview of fractal antenna engineering research,” *IEEE Trans. Antennas and Propagation*, vol. 45, no. 1, pp. 38–57, 2003.

[36] S. S. Mohammed, K. Ramasamy and T. Shanmuganantham, “A 2.45GHz sierpinski carpet edge-fed microstrip patch fractal antenna for WPT rectenna,” in *7th International Multi-Conference on Systems Signals and Devices (SSD)*, pp. 1–4, 2010.

[37] R. L. Vitale, “Design and prototype development of a wireless power transmission system for a micro air vehicle (MAV),” Master’s thesis, Naval Postgraduate School, 1999.

[38] L. M. M. Tan, “Efficient rectenna design for wireless power transmission for MAV applications,” Master’s thesis, Naval Postgraduate School, 2005.

[39] L. H. Toh, “A follow-up study on wireless power transmission for unmanned air vechicles,” Master’s thesis, Naval Postgraduate School, 2007.

[40] F. T. Ulaby, Eric Michielssen and Umberto Ravaioli, *Fundamentals of Applied Electromagnetics.* Upper Saddle River, NJ: Pearson, 2010.

[41] D. M. Pozar, *Microwave Engineering.* Hoboken, NJ: John Wiley & Sons, 1998.

[42] Anonymous RT/duroid® 5870/5880/5880LZ high frequency laminates datasheet, 2012.

[43] W. L. Stutzman and G. A. Thiele, *Antenna Theory and Design.* Hoboken, NJ: John Wiley & Sons, 1998.

[44] S. Makarov, A. Puzella and V. Iyer. Scan impedance for an infinite dipole array: Accurate theoretical model compared to numerical software. *Antennas and Propagation Magazine*, pp. 132–149, 2008.

INITIAL DISTRIBUTION LIST

1. Defense Technical Information Center
   Ft. Belvoir, Virginia

2. Dudley Knox Library
   Naval Postgraduate School
   Monterey, California

3. Dr. Dan C. Boger
   Chairman, Department of Information Science
   Naval Postgraduate School
   Monterey, California

4. Dr. Clark R. Robertson
   Chairman, Department of Electrical and Computer Engineering
   Naval Postgraduate School
   Monterey, California

5. Professor David C. Jenn
   Professor, Department of Electrical and Computer Engineering
   Naval Postgraduate School
   Monterey, California

6. Assistant Professor Ric Romero
   Professor, Department of Electrical and Computer Engineering
   Naval Postgraduate School
   Monterey, California

7. Robert D. Broadston
   Staff, Department of Electrical and Computer Engineering
   Naval Postgraduate School
   Monterey, California

8. Chung-Huan Huang
   Department of Information Science
   Naval Postgraduate School
   Monterey, California